AGU PUBLICATIONS

Geochemistry, Geophysics, Geosystems

RESEARCH ARTICLE
10.1002/2013GC005061

Key Points:
- Mantle can undergo melting at a step change in lithospheric thickness
- Samoan mantle may have been advected around the paleo-Tonga slab near present-day SPR
- New data support the hypothesis that Wallis Island has a Samoan pedigree

Supporting Information:
- Analytical Methods
- Readme text
- Figure S1
- Table S1

Correspondence to:
Allison A. Price,
price@umail.ucsb.edu

Citation:
Price, A. A., M. G. Jackson, J. Blichert-Toft, P. S. Hall, J. M. Sinton, M. D. Kurz, and J. Blusztajn (2014), Evidence for a broadly distributed Samoan-plume signature in the northern Lau and North Fiji Basins, *Geochem. Geophys. Geosyst.*, *15*, 986–1008, doi:10.1002/2013GC005061.

Received 26 SEP 2013
Accepted 30 DEC 2013
Accepted article online 4 JAN 2014
Published online 11 APR 2014

Evidence for a broadly distributed Samoan-plume signature in the northern Lau and North Fiji Basins

Allison A. Price[1], Matthew G. Jackson[1], Janne Blichert-Toft[2], Paul S. Hall[3], John M. Sinton[4], Mark D. Kurz[5], and Jerzy Blusztajn[6]

[1]Department of Earth Science, University of California, 1006 Webb Hall, Santa Barbara, California 93106, USA, [2]Laboratoire de Géologie de Lyon, Ecole Normale Supériere de Lyon and Université Claude Bernard Lyon 1, Lyon, France, [3]Department of Earth and Environment, Boston University, Boston, Massachusetts, USA, [4]School of Earth Ocean Science and Technology, University of Hawaii at Manoa, Honolulu, Hawaii, USA, [5]Department of Marine Chemistry, Woods Hole Oceanographic Institution, Woods Hole, Massachusetts, USA, [6]Department of Marine Geology and Geophysics, Woods Hole Oceanographic Institution, Woods Hole, Massachusetts, USA

Abstract Geochemical enrichment of lavas in the northern Lau Basin may reflect the influx of Samoan-plume mantle into the region. We report major and trace element abundances and He-Sr-Nd-Hf-Pb-isotopic measurements for 23 submarine volcanic glasses covering 10 locations in the northern Lau and North Fiji Basins, and for three samples from Wallis Island, which lies between Samoa and the Lau Basin. These data extend the western limit of geochemical observations in the Basins and improve the resolution of North-South variations in isotopic ratios. The Samoan hot spot track runs along the length of the northern trace of the Lau and North Fiji Basins. We find evidence for a Samoan-plume component in lavas as far West as South Pandora Ridge (SPR), North Fiji Basin. Isotopic signatures in SPR samples are similar to those found in Samoan Upolu shield lavas, but show a slight shift toward MORB-like compositions. We explain the origin of the enriched signatures by a model in which Samoan-plume material and ambient depleted mantle undergo decompression melting during upwelling after transiting from beneath the thick Pacific lithosphere to beneath the thin lithosphere in the northern Lau and North Fiji Basins. Other lavas found in the region with highly depleted isotopic signatures may represent isolated pockets of depleted mantle in the basins that evaded this enrichment process. We further find that mixing between the two components in our model, a variably degassed high-$^{3}He/^{4}He$ Samoan component and depleted MORB, can explain the diversity among geochemical data from the northern Lau Basin.

1. Introduction

Understanding how the upper mantle flows beneath the oceanic lithosphere is critical to deciphering mantle melting, the movement of tectonic plates, and the distribution and long-term evolution of geochemical reservoirs in the shallow mantle. The direction and rate of mantle flow is difficult to constrain, but spatial variations in the isotope geochemistry of oceanic lavas may provide hints for certain mantle flow patterns as well as the distribution of geochemical reservoirs in the mantle over time [e.g., *Zindler and Hart*, 1986; *Hofmann*, 1997; *White*, 2010].

Owing to the juxtaposition of the Tonga Trench and the Samoan hot spot (Figure 1), the Lau and North Fiji Basins provide a unique environment for the study of upper mantle flow around a subducting slab [*Hart et al*., 2004]. A wealth of both geochemical and geophysical evidence suggests that material from the Samoan hot spot is leaking southward into the adjacent Lau Basin, making this area ideal for mapping mantle flow on a regional scale [e.g., *Giardini and Woodhouse*, 1986; *Volpe et al*., 1988; *Gill and Whelan*, 1989b; *Poreda and Craig*, 1992; *Pearce et al*., 1995; *Ewart et al*., 1998; *Turner and Hawkesworth*, 1998; *Smith et al*., 2001; *Lupton et al*., 2009; *Escrig et al*., 2012]. First, the Samoan hot spot has various distinctive geochemical fingerprints (including high $^{3}He/^{4}He$ [up to 33.8 Ra, or ratio to the atmospheric value of 1.38×10^{-6}, *Jackson et al*., 2007a] or high $^{87}Sr/^{86}Sr$ [up to 0.72163, *Jackson et al*., 2007b, 2009]), which are readily recognizable from the isotopically distinct ambient mantle (e.g., low $^{3}He/^{4}He$ (8 Ra, ratio to atmosphere) and unradiogenic $^{87}Sr/^{86}Sr$) present beneath the Lau Basin [e.g., *Wright and White*, 1987; *Volpe et al*., 1988; *Farley et al*., 1992; *Poreda and Craig*, 1992; *Turner and Hawkesworth*, 1998; *Workman et al*., 2004; *Kelley et al*., 2006; *Langmuir et al*., 2006; *Falloon et al*., 2007; *Jackson et al*., 2007a, 2007b; *Escrig et al*., 2009, 2012].

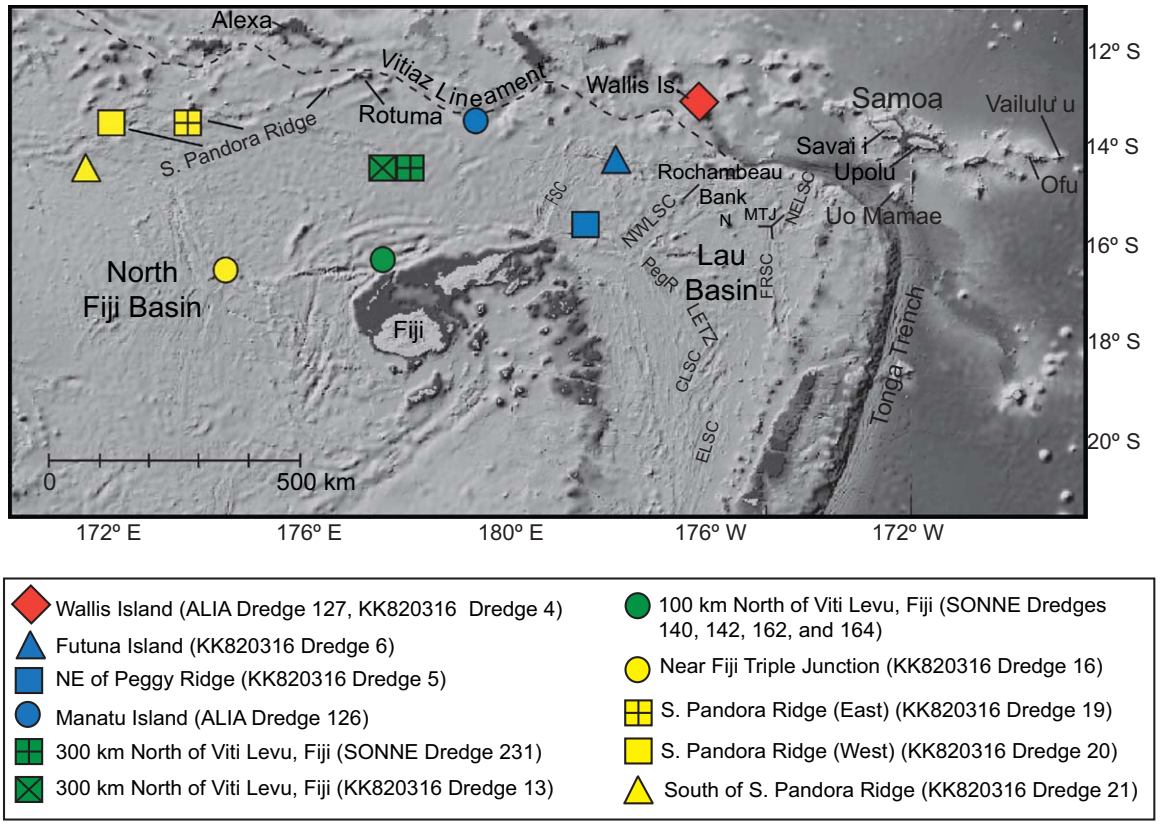

Figure 1. Map of the study region with locations of the samples analyzed in this study. Abbreviations: FSC, Futuna Spreading Center; NWLSC, Northwest Lau Spreading Center; PegR, Peggy Ridge; N, Niua fo'ou; MTJ, Mangatolu (King's) Triple Junction; NELSC, Northeast Lau Spreading Center; FRSC, Fonualei Rift and Spreading Center; LETZ, Lau Extensional Transform Zone; CLSC, Central Lau Spreading Center; ELSC, Eastern Lau Spreading Center. Base map was created using GeoMapApp (http://www.geomapapp.org) with topographic and bathymetric data from SRTM_PLUS (Becker et al., 2009, v. 5.0)

Second, the density and distribution of young volcanism within the Lau Basin provides excellent spatial sampling of the shallow upper mantle.

Isotopic evidence for the distribution of Samoan-plume mantle beneath the Lau Basin takes several forms. Elevated $^{3}He/^{4}He$ ratios (up to 28 Ra*; Lupton et al.* [2009]) that are rarely found in back arc basins [*Macpherson et al.*, 1998; *Shaw et al.*, 2004] have been observed in the northwest region of the Lau Basin (e.g., Rochambeau Bank, Rochambeau Rifts, and the Northwest Lau Spreading Center). These high-$^{3}He/^{4}He$ ratios strongly suggest the presence of plume material in the region [*Poreda and Craig*, 1992; *Honda et al.*, 1993; *Lupton et al.*, 2009; *Tian et al.*, 2011; *Hahm et al.*, 2012; *Lytle et al.*, 2012]. If the Samoan plume is the source of the He-isotopic anomaly, the northern, southern, and eastern extent of Samoan-plume incursion into the Lau Basin can be mapped from the spatial distribution of igneous rocks with high $^{3}He/^{4}He$ [*Poreda and Craig*, 1992; *Hilton et al.*, 1993; *Honda et al.*, 1993; *Lupton et al.*, 2009].

However, high-$^{3}He/^{4}He$ (>20 Ra) signatures are rare, even in Samoan lavas. Therefore, other geochemical signatures unique to Samoan lavas, including highly radiogenic $^{87}Sr/^{86}Sr$ and telltale EM2 Pb-isotopic compositions [e.g., *Wright and White*, 1987; *Farley et al.*, 1992; *Workman et al.*, 2004; *Jackson et al.*, 2007a, 2007b] in lavas with low $^{3}He/^{4}He$ can also be useful for detecting a Samoan component [e.g., *Volpe et al.*, 1988; *Gill and Whelan*, 1989a; *Poreda and Craig*, 1992; *Wendt et al.*, 1997; *Ewart et al.*, 1998; *Pearce et al.*, 2007; *Falloon et al.*, 2007; *Regelous et al.*, 2008; *Escrig et al.*, 2009; *Jackson et al.*, 2010; *Lytle et al.*, 2012; *Escrig et al.*, 2012], if it exists in the region. Owing to a paucity of geochemical and isotopic data for lavas from the northwestern Lau and northern North Fiji Basins, the western boundary and distribution of Samoan-plume material in the region is not well known. While the flow may be characterized by a narrow, finger-like intrusion, as proposed by *Turner and Hawkesworth* [1998], it could also take the form of a broad anomaly more consistent with simple lateral spreading of ponded Samoan-plume mantle at the base of the lithosphere [e.g., *Sleep*, 1996]. The Samoan hot spot tracks runs along the length of the northern trace of

the Lau and North Fiji Basins. If Samoan-plume mantle material has ponded and spread both laterally and to the south, its presence would be detected in the basins further to the west.

Here, we use a combination of geochemical data from northern Lau and North Fiji Basin lavas to constrain the spatial distribution of Samoan mantle source material in the region. Broadening the field area of geochemically characterized lavas to the west helps define the western boundary of Samoan-plume material influence. We present new Sr, Nd, Pb, Hf, and He-isotopic data, together with major and trace element concentrations, on samples from 11 locations along a swath covering the northern region of the Lau and North Fiji Basins, as well as Wallis Island (see supporting information for analytical methods and discussion). The new data suggest that the influence of the Samoan plume extends into the North Fiji Basin (at least 1400 km west of the current location of the youngest active Samoan volcano, Vailulu'u; *Hart et al*. [2000]).

1.1. Geologic Setting

The Samoan archipelago is an age progressive group of volcanic islands constituting a hot spot track [e.g., *Duncan*, 1985; *Hart et al*., 2004; *Koppers et al*., 2008; *McDougall*, 2010; *Koppers et al*., 2011]. The origin of volcanism in Samoa is complicated by its proximity to the northern terminus of the Tonga Trench, located just over 100 km south of the Samoan island of Savai'i. Lithospheric cracking caused by tectonic stresses related to the nearby trench was suggested to enhance melting and melt extraction at Samoa, and this model is in part supported by the observation that Savai'i Island has been completely resurfaced with a veneer of young (<1 Ma) rejuvenated lavas [e.g., *Hawkins and Natland*, 1975; *Natland and Turner*, 1985; *Natland*, 2003; *Konter and Jackson*, 2012]. However, geochronological data for lavas recovered from the deep submarine flanks of Savai'i indicate a 5.0 Ma eruption age, at which time the Tonga Trench was positioned ~1400 km to the west of Savai'i and well out-of-range to influence shield-building volcanism at the island [*Koppers et al*., 2008]. While this early volcanism at Savai'i was not triggered by tectonic stresses, rejuvenated volcanism on Savai'i during the past 1 Ma, as well as on Wallis Island and Lalla Rookh seamount, may have been enhanced by tectonic stresses from the trench [*Price and Kroenke*, 1991; *Hart et al*., 2004; *Konter and Jackson*, 2012].

The trace of the Samoan hot spot, which is anchored by Vailulu'u seamount in the east, runs parallel to the northern border of the Lau and North Fiji Basins, and is separated from these basins by the Vitiaz Lineament (Figures 1 and 2). The Lau and North Fiji Basins are located between the Pacific and Indo-Australian plates. The region is flanked by two subduction zones that face each other and form the Tonga Trench by the westward subduction of the Pacific plate, and the Vanuatu Trench by subduction of the Indo-Australian plate under the North Fiji Basin. Due to trench rollback, the northern terminus of the Tonga Trench is moving eastward at ~170 mm/yr, while the Pacific plate is moving westward at ~70 mm/yr, resulting in a total convergence rate that is the fastest on Earth, at ~240 mm/yr [*Bevis et al*., 1995]. North of this terminus, the Pacific plate tears [*Millen and Hamburger*, 1998; *Govers and Wortel*, 2005] and, instead of subducting into the trench, the Pacific plate continues to the west. This tearing is thought to generate the stresses that give rise to abundant rejuvenated volcanism in Samoa [*Konter and Jackson*, 2012]. To the south of the terminus, the Pacific plate subducts into the Tonga Trench, resulting in the opening of a "slab window" which allows Samoan mantle to flow southward into the shallow mantle in the Lau Basin [e.g., *Turner and Hawkesworth*, 1998; Figure 2]. This slab window may have begun opening at 4.5 Ma, when the terminus was located further to the west, just south of Alexa seamount [*Hart et al*., 2004]. If so, material from the Samoan hot spot may have been advected into these basins for the past 4.5 Ma.

The Vitiaz Lineament marks the boundary between the old (~100 Ma) Pacific lithosphere and the young (<5 Ma) lithosphere of the Lau and North Fiji Basins [*Brocher*, 1985; *Pelletier and Auzende*, 1996]. *Hart et al*. [2004] suggested that the segment of the Vitiaz Lineament east of 180°W was formed by the propagation of the tear in the Pacific plate, while the Tonga Trench swept eastward toward the active end of the Samoan hot spot over the last 4–5 Ma (Figure 2). However, the entire length of the Vitiaz Lineament has also been suggested to be a pre-Tongan "fossil" subduction zone marking the location of subduction of the Pacific plate under the Australian plate until ~12 Ma, at which time the Ontong-Java plateau collided with the trench, halting subduction along the Vitiaz Lineament [e.g., *Brocher*, 1985; *Yan and Kroenke*, 1993; *Auzende et al*., 1995; *Pelletier and Auzende*, 1996; *Pearce et al*., 2007]. If so, the high density of islands and seamounts to the south of the Vitiaz Lineament may be the product of arc volcanism. Nonetheless, at least three volcanoes along the southern border of the Vitiaz Lineament—Rotuma Island, Manatu seamount,

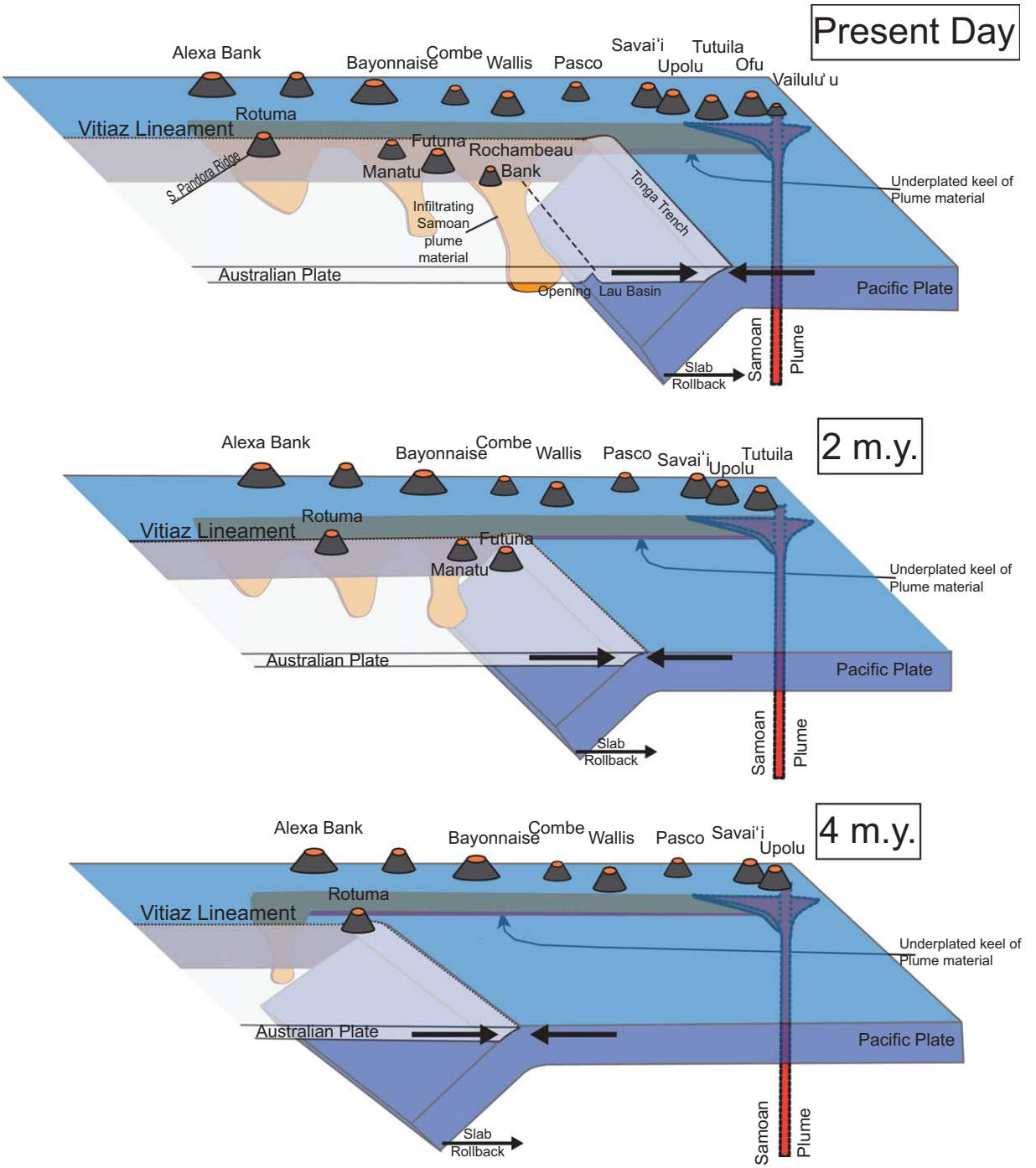

Figure 2. Cartoon schematic showing the tectonic evolution of the Lau and North Fiji Basins over the past 4 million years. The tectonic reconstruction is based on the model proposed by *Hart et al*. [2004]. The cartoon is a three-dimensional adaptation of Figure 9 from *Hart et al*. [2004]. We do not show Futuna and Manatu at the 4 Ma time step owing to complications with the plate reconstruction as discussed in *Hart et al*. [2004]. Incorporation of underplated Samoan-plume material during toroidal flow around the Tonga slab is suggested to have occurred for the past 4 Ma, as the Tonga trench has migrated to the east relative to the Samoan hot spot. It is unknown if "tongues" of Samoan material are currently flowing into the North Fiji Basin; however, they likely did in the past when the Tonga trench was located further to the west.

and Futuna Island—host lavas with ages that postdate Vitiaz Lineament subduction (all ages are Quaternary to 4.9 Ma) [*Duncan*, 1985; *Woodhall*, 1987]. Furthermore, Rotuma lacks arc-like geochemical characteristics [*Hart et al*., 2004] and we show that Manatu and young Futuna lavas from this study also appear to lack arc-like affinities (section 3).

Prior to subduction cessation, the Vitiaz Trench marked a continuous subduction zone from the Solomons to Tonga, with west to southwest subduction of the Pacific plate under the Indian lithosphere. The Vitiaz Trench was composed of the older pieces of the Tonga-Fiji-Vanuatu and Solomon arcs [e.g., *Gill*, 1984; *Gill and Whelan*, 1989b; *Begg and Gray*, 2002; *Crawford et al*., 2003; *Pearce et al*., 2007]. When subduction ceased along the Vitiaz Trench, the boundary is thought to have become a transform [e.g., *Pelletier and Auzende*, 1996] and the remnant slab detached. However, GPS data from Rotuma and Futuna Islands—both located just south of the Vitiaz Lineament—show that they are moving with the Pacific plate [*Calmant et al*., 2003], indicating that little or no transform motion along the Vitiaz Lineament is occurring at present [*Hart et al*., 2004]. The Vitiaz Lineament, therefore, may be a fossil boundary and any transcurrent motion between the Australian and Pacific plates occurs south of the boundary along transform faults in the Lau Basin [*Hart et al*., 2004].

1.2. Previous Geochemical Work in the Northern Lau Basin

Several previous studies have shown that quaternary volcanism with signatures similar to ocean island basalts (OIB) is pervasive throughout the Lau and North Fiji Basins, but the origins, and possible relationships with Samoa remain unknown. *Gill and Whelan* [1989a, 1989b] showed that Fijian lavas became OIB-like by 3 Ma. *Poreda and Craig* [1992] were the first to show elevated $^{3}He/^{4}He$ isotopes at Rochambeau Bank, in the northwest Lau Basin. These Samoan-like signatures were used to suggest the mixing of a Samoan component with ambient depleted mantle. *Honda et al*. [1993] reported moderately low $^{3}He/^{4}He$ in the Eastern and Central Lau Spreading Centers as well as the Mangatolu Triple Junction. Using this information, *Turner and Hawkesworth* [1998] refined the hypothesis of *Poreda and Craig* [1992] and suggested a model that included a "finger-like" intrusion of Samoan mantle material into the northern Lau Basin. More recently, *Lupton et al*. [2009] found that many locations within the northern Lau Basin have high $^{3}He/^{4}He$, but that these values do not clearly correlate with ridge configuration or latitude, although the highest $^{3}He/^{4}He$ values do cluster in the northernmost region of the Lau Basin. Further studies by *Lupton et al*. [2012], *Hahm et al*. [2012], and *Peto et al*. [2013] show that Ne-isotopes correlate with He isotopes, supporting the hypothesis of a Samoan-plume influence in the region. Working on the same samples as *Lupton et al*. [2009], *Jenner et al*. [2012] found enrichment of Cu and Ag in lavas from the Northwest and Central Lau Spreading Centers and Rochambeau Rifts, and argued that the data may require a different high-Cu source, as Samoan lavas and MORB do not have high-Cu abundances. Nonetheless, the study argues for the presence of a Samoan plume component in the region. Isotopic, major element, and volatile data were added by *Lytle et al*. [2012], who suggested the possibility of a second unidentified mantle plume to the west of the Northwest Lau Spreading Center. *Tian et al*. [2008, 2011] provided new Sr-Nd isotope and trace element data from Rochambeau Bank, Peggy Ridge, Mangatolu Triple Junction, Niuafou'ou, and both the Central and Eastern Lau Spreading Centers, while *Hahm et al*. [2012] analyzed volatiles and noble gases in these samples. Their data provide evidence of influence for both subduction-related and OIB components. Despite the number of studies conducted in the Lau Basin, there is little data from the North Fiji Basin. Here, we provide a full suite of major and trace element and isotopic data for samples recovered from the northern Lau and North Fiji Basin (Figure 1). We use these data to assess the mantle sources in the region.

2. Sample Locations and Descriptions

The locations for all new samples presented in this study are shown in Figure 1 and presented in Table 1. The 26 basaltic submarine dredge samples recovered from the northwestern Lau and North Fiji Basins and Wallis Island were obtained from three dredging expeditions: two legs of the R/V Kana Keoki cruise KK820316 in 1982 [*Sinton et al*., 1985; *Johnson et al*., 1986; *Sinton et al*., 1993]; cruise 35/3 of the German research vessel R/V Sonne in 1985 [*Johnson and Sinton*, 1990]; the ALIA 2005 cruise aboard the R/V Kilo Moana [*Jackson et al*., 2007b; *Koppers et al*., 2008; *Jackson et al*., 2010; *Koppers et al*., 2011]. The dredge sites are divided into three regions across the Lau and North Fiji Basins and two sample localities at Wallis Island.

2.1. Dredges in the North Fiji Basin

We examine samples from four different dredge sites in the North Fiji Basin. Two different dredges (dredges 19 and 20) were made on South Pandora Ridge (SPR), and these are shown separately in all figures. Dredge 19 consisted of fresh glassy pillow lava fragments with slight surface alteration [*Sinton et al*., 1993]. Dredge 20 contained extremely fresh glassy pillow fragments with no visible alteration [*Sinton et al*.,

AGU Geochemistry, Geophysics, Geosystems

10.1002/2013GC005061

Table 1. Major Element Compositions of Lavas Examined in This Study

Sample Name	Location	Cruise	Lon.	Lat.	Age	SiO_2	TiO_2	Al_2O_3	FeO_{tot}	MnO	MgO	CaO	Na_2O	K_2O	P_2O_5	Total	Mg#[a]	Method
140-1A glass	N of Fiji, 100 km N of Viti Levu	Sonne	−16.417	177.417	<0.5 Ma[b]	55.23	1.76	14.34	10.89	0.21	3.65	7.92	3.56	0.34	0.21	98.11	0.41	EMP[b]
142-1 glass	N of Fiji, 100 km N of Viti Levu	Sonne	−16.417	177.417	<0.5 Ma[b]	50.12	1.61	15.86	9.47	0.16	7.53	11.39	2.78	0.30	0.17	99.39	0.63	EMP[b]
162-1 glass	N of Fiji, 100 km N of Viti Levu	Sonne	−16.417	177.417	<0.5 Ma[b]	50.04	0.75	16.38	8.56	0.16	9.16	13.16	1.94	0.05	0.06	100.26	0.69	EMP[b]
164-1 glass	N of Fiji, 100 km N of Viti Levu	Sonne	−16.417	177.417	<0.5 Ma[b]	53.84	1.75	14.69	10.36	0.20	4.19	8.31	3.61	0.57	0.29	97.81	0.46	EMP[b]
231-1A glass	N of Fiji, 300 km N of Viti Levu	Sonne	−14.480	177.687		50.34	2.49	12.48	16.24	0.29	5.03	9.47	3.05	0.19	0.21	99.79	0.39	EMP[b]
13-2 glass	N of Fiji, 300 km N of Viti Levu	KK820316	−14.480	177.687	1–2 Ma[c]	50.80	2.08	13.28	13.99	0.18	5.97	10.94	2.71	0.19	0.21	100.35	0.47	EMP[c]
13-4 glass	N of Fiji, 300 km N of Viti Levu	KK820316	−14.480	177.687	1–2 Ma[c]	51.02	2.00	13.29	13.74	0.22	6.17	10.77	2.77	0.17	0.22	100.37	0.49	EMP[c]
126-18 glass	N. Fiji Basin, Manatu	ALIA	−13.368	179.277	4.36 Ma[d]													
127-05 glass	Wallis Island	ALIA	−13.085	−176.210														
127-05 powder	Wallis Island	ALIA	−13.085	−176.210		47.05	1.82	13.48	11.60	0.18	13.01	9.14	2.59	0.92	0.20	100.00	0.70	XRF[e]
127-11 glass	Wallis Island	ALIA	−13.085	−176.210														
127-11 powder	Wallis Island	ALIA	−13.085	−176.210		47.63	1.93	14.17	11.12	0.16	11.43	9.63	2.73	0.99	0.21	100.00	0.68	XRF[e]
4-1 glass	Wallis Island	KK820316	−13.085	−176.210	0.08-0.8 Ma[f,g]	47.48	2.36	15.96	10.46	0.12	5.95	11.02	3.33	1.26	0.34	98.28	0.54	EMP[h]
5–14 glass	N. Lau Basin, NE Peggy Ridge	KK820316	−15.658	−178.495	1.4 Ma[g]	49.53	2.11	15.48	10.29	0.19	6.46	10.94	3.01	0.20	0.22	98.43	0.57	EMP[c]
5–15 glass	N. Lau Basin, NE Peggy Ridge	KK820316	−15.658	−178.495	1.4 Ma[g]	49.16	2.01	15.14	10.78	0.18	7.45	10.68	2.90	0.19	0.21	98.70	0.59	EMP[c]
5–19 glass	N. Lau Basin, NE Peggy Ridge	KK820316	−15.658	−178.495	1.4 Ma[g]	49.54	2.07	15.34	10.51	0.20	6.71	10.75	3.07	0.21	0.20	98.60	0.57	EMP[c]
6–14 glass	N. Lau Basin, Futuna	KK820316	−14.402	−177.875	4.9 Ma[g]	50.09	1.09	14.29	10.45	0.18	7.53	12.40	2.51	0.07	0.13	98.74	0.60	EMP[i]
6–52 glass	N. Lau Basin, Futuna	KK820316	−14.402	−177.875	4.9 Ma[g]	52.83	1.16	16.16	8.29	0.09	7.85	10.29	2.46	0.11	0.17	99.41	0.67	EMP[i]
6–52 powder	N. Lau Basin, Futuna	KK820316	−14.402	−177.875	4.9 Ma[g]	51.98	1.06	14.95	8.64	0.14	11.13	9.47	2.43	0.11	0.10	99.62	0.73	XRF[e]
6–54 glass	N. Lau Basin, Futuna	KK820316	−14.402	−177.875	4.9 Ma[g]	53.28	0.97	16.11	8.30	0.17	8.10	10.67	2.43	0.10	0.14	100.27	0.67	EMP[i]
16-12 glass	N. Fiji Basin, Near Fiji Triple Junct.	KK820316	−16.612	174.273	0.1–1 Ma[c]	49.61	1.26	16.49	9.79	0.16	8.38	12.09	2.65	0.09	0.19	100.71	0.64	EMP[c]
16-14 glass	N. Fiji Basin, Near Fiji Triple Junct.	KK820316	−16.612	174.273	0.1–1 Ma[c]	49.09	1.29	16.83	9.59	0.11	8.91	12.46	2.61	0.05	0.16	101.10	0.66	EMP[c]
19-1 glass	N. Fiji Basin, S. Pandora Ridge	KK820316	−13.543	173.477	<50 ka[c]	50.48	2.03	15.92	9.90	0.14	6.56	10.92	3.10	0.66	0.29	100.00	0.58	EMP[c]
19-2 glass	N. Fiji Basin, S. Pandora Ridge	KK820316	−13.543	173.477	<50 ka[c]	50.60	1.95	15.98	9.95	0.16	6.35	10.87	3.00	0.69	0.30	99.85	0.57	EMP[c]
19-7 glass	N. Fiji Basin, S. Pandora Ridge	KK820316	−13.543	173.477	<50 ka[c]	49.25	2.04	15.85	10.13	0.16	6.41	10.93	3.00	0.68	0.21	98.66	0.57	EMP[c]
20-2 glass	N. Fiji Basin, S. Pandora Ridge	KK820316	−13.517	171.973	<50 ka[c]	49.19	2.07	16.44	8.78	0.07	6.12	10.95	2.96	0.83	0.27	97.68	0.59	EMP[c]
20-3 glass	N. Fiji Basin, S. Pandora Ridge	KK820316	−13.517	171.973	<50 ka[c]	49.80	2.16	16.23	8.79	0.13	6.29	10.76	3.00	0.81	0.28	98.25	0.60	EMP[c]
20-16 glass	N. Fiji Basin, S. Pandora Ridge	KK820316	−13.517	171.973	<50 ka[c]	48.87	2.08	16.37	8.76	0.12	6.16	10.79	2.97	0.88	0.36	97.36	0.60	EMP[c]
21-1 glass	N. Fiji Basin, S of S. Pandora Ridge	KK820316	−14.552	171.470	>2 Ma[c]	49.39	0.96	16.17	9.37	0.13	9.29	11.98	2.17	0.05	0.16	99.67	0.68	EMP[c]

[a]Mg# = molar ratio of MgO/(MgO + 0.85 × FeO).

[b]Data are from *Johnson and Sinton* [1990]. Ages are estimated by the age of onset of regional spreading. Major elements were measured by a fully automated Cameca three spectrometer wavelength dispersive microprobe (EMP) at the Hawaii Institute of Geophysics.

[c]Data are from *Sinton et al.* [1993]. Ages are estimated based on degree of weathering and Mn crust thickness. Major elements were measured by a fully automated Cameca three spectrometer wavelength dispersive microprobe (EMP) at the Hawaii Institute of Geophysics.

[d]$^{40}Ar/^{39}Ar$ age is from *Koppers et al.* [2011].

[e]Data from *Jackson et al.* [2010]. Major elements were measured by X-ray fluorescence (XRF) on a ThermoARL XRF at Washington State University (WSU).

[f]K/Ar age is from *Price et al.* [1991].

[g]K/Ar and $^{40}Ar/^{39}Ar$ ages are from *Duncan* [1985].

[h]Data from *Johnson et al.* [1986]. Major elements were measured by a fully automated Cameca three wavelength dispersive microprobe (EMP) at the Hawaii Institute of Geophysics.

[i]Data from *Sinton et al.* [1985]. Major elements were measured by a fully automated Cameca three wavelength dispersive microprobe (EMP) at the Hawaii Institute of Geophysics.

1993]. Dredge 21 was recovered ~100 km south of SPR on a west-northwest striking ridge. The single sample from this dredge is a nearly aphyric pillow fragment with a brown weathered surface and a thin Mn crust [*Sinton et al*., 1993]. A fourth dredge (dredge 16) was made further to the south in the North Fiji Basin on a southeast facing, ~1000 m escarpment, located near the North Fiji Basin triple junction. The two samples from dredge 16 are olivine-phyric, plagioclase microphyric pillow basalts with thin, 1 mm Mn crusts.

2.2. Dredges North of Fiji

Samples from seven different dredge sites in the region north of the Fijian Islands are divided geographically into two groups. The first group consists of four different dredges made in a tightly clustered region (within ~10 km) ~100 km north of Viti Levu, Fiji. These dredges sampled the spreading centers in the area. All samples are extremely fresh and therefore likely to be quite young in age [*Johnson and Sinton*, 1990]. The second group consists of two different dredges made in close proximity ~300 km north of Viti Levu, Fiji (sample 231-1A and dredge 13). Dredge 231 was made on the Southern Central Ridge, North Fiji Basin [*Johnson and Sinton*, 1990]. Dredge 13 was made about 15–20 km inside a pseudofault in what may be a now-defunct part of a propagating rift system [*Brocher*, 1985]. Dredge 13 was composed of pillow fragments with 2 mm Mn crusts [*Sinton et al*., 1993].

2.3. Dredges in the Northern Lau Basin

We analyzed samples from three different dredge sites in the northern Lau Basin: Manatu Seamount (dredge 126), Futuna Island (dredge 6), and the region just to the northeast of Peggy Ridge (dredge 5). Two different samples from different dredge sites at Manatu have been dated at 1.8 Ma [*Duncan*, 1985; *Sinton et al*., 1985] and 4.36 Ma [*Koppers et al*., 2011], while the single sample from Futuna has an age of 4.9 Ma [*Duncan*, 1985]. The samples dredged northeast of Peggy Ridge are relatively old (1.4 Ma) [*Duncan*, 1985] and therefore were collected outside the region of active extrusion [*Sinton et al*., 1985].

2.4. Wallis Island

We analyzed samples from two different dredge sites (dredges 127 and 4). All of the Wallis dredge samples are extremely fresh and likely as young as subaerial lavas from Wallis Island (0.08–0.8 Ma) [*Duncan*, 1985; *Price and Kroenke*, 1991].

3. Results

3.1. Major Element Geochemistry

The samples examined in this study range from basaltic to basaltic andesite in composition (Figure 3). The alkali-tholeiite division [*Macdonald and Katsura*, 1964] shows that only the Wallis Island samples are alkalic. This is expected if Wallis Island and Samoa share a genetic relationship (see section 4.4), as almost all lavas associated with the Samoan hot spot are alkali basalts [*Natland and Turner*, 1985; *Workman et al*., 2004; *Jackson et al*., 2010]. Both dredges of SPR yielded glasses that are near the alkali tholeiite division. Because SPR is anchored on the northeast by Rotuma Island, which is host to alkali volcanics [*Woodhall*, 1987], it is not surprising that SPR basalts are transitional in composition. All other lavas examined in this study plot within the tholeiitic field in Figure 3.

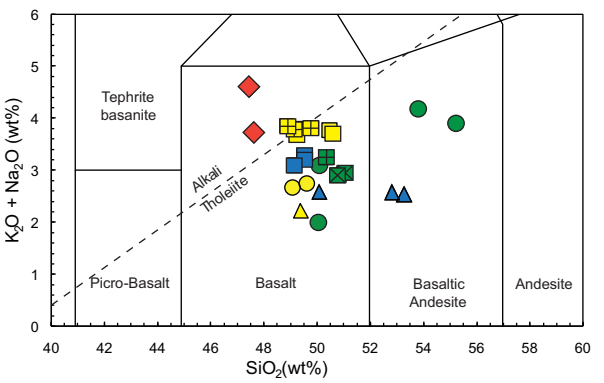

Figure 3. Silica versus total alkali plot, with subdivisions for different rock classifications based on *Le Bas et al*. [1986]. The alkali-tholeiite line is from *Macdonald and Katsura* [1964]. Symbols are the same as in Figure 1.

3.2. Trace Element Geochemistry

The lavas examined in this study exhibit a wide range of trace element abundances. We show these variations in primitive mantle-normalized plots (spidergrams) (Figure 4 and Table 3). The only true alkali basalts from this study, all from Wallis Island,

have the highest overall concentrations of the most incompatible trace elements. The shape of the spidergrams for the three Wallis Island samples are broadly similar, but sample 4-1 from the KK820316 cruise has higher concentrations of incompatible elements than samples 127-05 and 127-11 from the ALIA 2005 cruise (Table 2 and Figure 4). Sample 4-1 has lower whole rock MgO (5.95 wt. %) than samples 127-05 and 127-11 (whole rock MgO is 13.01 and 11.43 wt. %, respectively). Additionally, trace element measurements of both glass and whole rock powder from sample 127-05 show a whole rock pattern which is shifted to lower normalized concentrations than the glass for all elements, except for U, K, and Pb. The slight enrichment of these elements in the whole rock may be explained by the fact that they are mobile and become enriched in altered portions of the whole rock, but not in fresh glass.

Wallis Island lies downstream of the Samoan hot spot, but a genetic relationship between the two remains uncertain [*Price et al*., 1991; *Jackson et al*., 2010] as Wallis Island lavas are 0.08–0.8 Ma (Table 1), too young to fit the Samoan hot spot age progression [*Koppers et al*., 2011]. If Wallis Island lavas are Samoan, they must belong to a late rejuvenated stage. Samoan rejuvenated lavas are enriched in Ba relative to other elements of similar compatibility, and thus exhibit higher Ba/Sm and Ba/Th ratios relative to Samoan shield-stage lavas [*Jackson et al*., 2010]. In a plot of Ba/Sm versus Ba/Th, Wallis Island lavas fall within the Samoan rejuvenated field, which is defined by subaerial rejuvenated lavas in the eastern Samoan volcanic province (ESAM) (Figure 5). Trace element spidergrams of Wallis Island plot together with patterns for Samoan rejuvenated lavas from Savai'i and Upolu Islands (Figure 4).

SPR samples are also incompatible element enriched, and they are geochemically similar to Samoan Upolu shield lavas. However, SPR lavas have lower trace element abundances for elements more incompatible than Tb. The slope of trace elements less incompatible than Tb in the spidergrams (Figure 4) is shallower for SPR lavas than Upolu lavas, suggesting that the SPR lavas have a weaker garnet signature than Upolu lavas. Nonetheless, the SPR patterns are similar to the Upolu patterns, especially for the most incompatible elements (Rb through Nd) (Figure 4).

Two nonridge volcanoes located south of the Vitiaz Lineament—Manatu seamount and Futuna Island—were previously suggested to exhibit possible arc-like signatures owing to the "jagged" nature of trace element pattern observed in some of the whole rock measurements [*Jackson et al*., 2010]. However, the elements that exhibit the largest spikes, or anomalies, on the Manatu and Futuna patterns are K, U, and Rb (Figure 4), which are all fluid mobile and susceptible to modification during submarine alteration. The trace element data on fresh glasses from these two volcanoes exhibit relatively smooth patterns, with none of the anomalous enrichments or depletions in K, U, and Rb visible in the whole rock analyses. Rather than showing evidence of arc influence, the patterns for the Manatu and some of the Futuna glass samples from this study are similar to average MORB tholeiites. Finally, we note that a subset of Futuna lavas are strongly depleted in both the heavy rare earth elements (HREE) and the most incompatible elements, giving a distinct "hump" shape to the spiderdiagram.

The four dredges taken in close proximity ~100 km north of Viti Levu, Fiji, have a surprising diversity of trace element abundances and spidergram shapes. Sample 142-1 has a slight garnet signature ($La_N/Lu_N = 1.8$), while its spidergram shows positive Nb and Ta anomalies and a negative U anomaly. Sample 164-1 also has a slight garnet signature ($La_N/Lu_N = 1.8$), but it lacks the positive Nb and Ta anomalies and the negative U anomaly that characterize 142-1. However, sample 164-1 does have moderate positive Zr and Hf anomalies. Sample 140-1A has a relatively flat spidergram pattern ($La_N/Lu_N = 1.2$), with no evidence for a garnet signature; it exhibits dramatic positive Zr and Hf anomalies and positive U and Th anomalies. Finally, sample 162-1 is one of the most incompatible element-depleted samples in this study ($La_N/Lu_N = 0.40$), with Rb, Ba, and Th concentrations that are only 1.3–1.5 times the primitive mantle values. This sample also has the most geochemically depleted Sr, Nd, and Hf-isotopic signatures in this study (see section 3.3).

The sample taken from ~100 km south of SPR (21-1; $La_N/Lu_N = 0.60$) and the two samples from north of the North Fiji Basin triple junction (16-12 and 16-14; $La_N/Lu_N = 0.66$ and 0.56, respectively) are similarly incompatible element depleted and have patterns that are generally similar to sample 162-1. Samples from ~300 km north of Viti Levu, Fiji, 231-1A ($La_N/Lu_N = 0.71$) and 13-4 and 13-2 ($La_N/Lu_N = 0.77$ and 0.76, respectively) also have incompatible element-depleted spidergrams, but have higher overall trace element abundances than other lavas with incompatible element-depleted patterns from the region. Sample 231-1A has Lu concentrations nearly 20 times the primitive mantle values, while Lu in sample 162-1 is only about five times higher than primitive mantle.

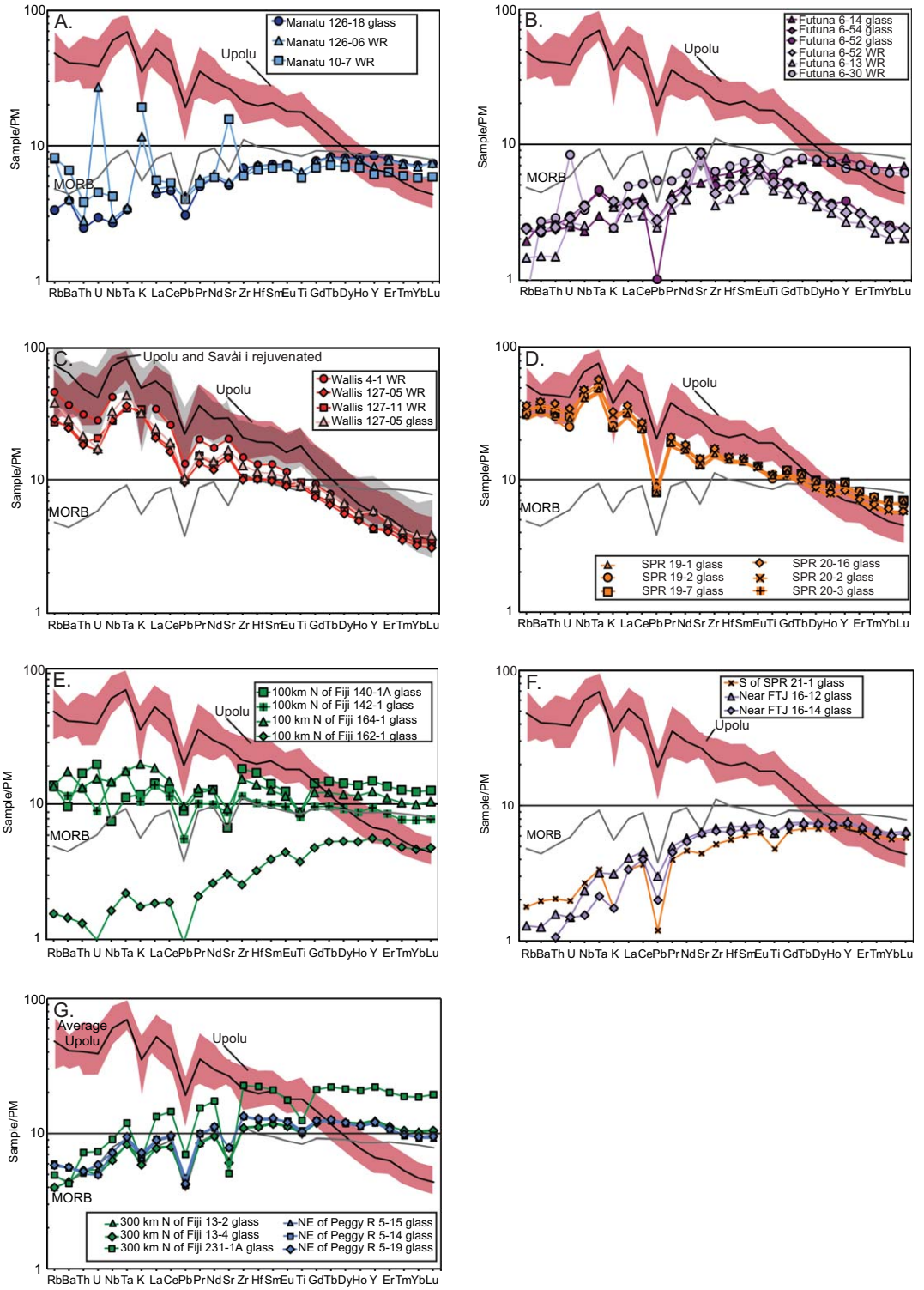

Figure 4. Primitive mantle-normalized trace element patterns for the lavas examined in this study. Abbreviations: Peggy R, Peggy Ridge; SPR, South Pandora Ridge; FTJ, Fiji Triple Junction. Previously published data on whole rock powders from Manatu, Futuna, and Wallis Island [*Jackson et al*., 2010] are compared with 24 glasses and one whole rock powder from this study. The "spiky" patterns in the whole rock data of Manatu and Futuna [*Jackson et al*., 2010], caused by enrichments in K, U, and Rb, contrast with the smooth patterns observed in the fresh glasses for these locations (this study), suggesting alteration of the whole rocks published by *Jackson et al*. [2010]. The three samples from northeast of Peggy Ridge have similar trace element abundances and are nearly indistinguishable from each other in this plot. Average Upolu, which was calculated from Upolu shield data with MgO > 6.5 wt. %, is shown on all plots as a black line. The span of Upolu shield lavas with MgO > 6.5 wt. % is shown with the red field in all plots. (c) also shows the span of Upolu and Savai'i rejuvenated lavas with MgO > 6.5 wt. % [*Hauri and Hart*, 1993; *Workman et al*., 2004]. Average MORB is from *Gale et al*. [2013] and is plotted as a gray line in all plots. The primitive mantle composition is from *McDonough and Sun* [1995]. All trace element data used in this plot, including data used to construct the data fields, were measured by ICP-MS.

AGU Geochemistry, Geophysics, Geosystems

10.1002/2013GC005061

Table 2. Trace Element Analyses of Lavas Reported in This Study

Sample Name	Method	Rb	Ba	Th	U	Nb	Ta	La	Ce	Pb	Pr	Nd	Sr	Zr	Hf	Sm	Eu	Gd	Tb	Dy	Ho	Y	Er	Tm	Yb	Lu
140-1A glass	ICP-MS	8.20	63.4	1.34	0.40	4.94	0.41	9.21	21.6	1.34	3.07	15.9	133.2	191.4	4.79	5.70	1.91	7.72	1.45	9.55	2.05	63.8	5.92	0.87	5.40	0.85
142-1 glass	ICP-MS	7.96	75.5	1.03	0.18	9.40	0.64	8.87	19.0	0.82	2.55	12.4	172.7	119.7	2.88	4.00	1.46	5.18	0.95	6.18	1.30	40.2	3.70	0.52	3.34	0.52
162-1 glass	ICP-MS	0.92	9.5	0.10	0.02	1.07	0.08	1.19	3.14	0.14	0.53	3.23	59.9	26.5	0.90	1.58	0.68	2.57	0.52	3.57	0.78	24.0	2.27	0.32	2.03	0.32
164-1 glass	ICP-MS	8.13	114.0	1.04	0.31	9.59	0.64	11.9	24.7	1.44	3.29	15.8	183.3	160.0	3.92	5.11	1.76	6.60	1.20	7.86	1.71	53.0	4.81	0.69	4.36	0.70
231-1A glass	ICP-MS	2.97	28.3	0.58	0.15	5.97	0.44	8.64	24.3	1.05	3.90	21.6	101.2	238.0	6.26	8.46	2.72	11.51	2.18	14.38	3.08	94.9	8.81	1.28	8.21	1.30
13-2 glass	ICP-MS	2.40	29.2	0.42	0.11	4.25	0.31	5.14	13.6	0.63	2.17	12.2	125.0	116.9	3.21	4.84	1.76	6.68	1.24	8.14	1.78	53.9	4.95	0.71	4.56	0.72
13-4 glass	ICP-MS	2.39	29.0	0.42	0.10	4.17	0.31	5.01	13.3	0.62	2.15	12.0	120.6	114.4	3.15	4.74	1.72	6.48	1.24	8.07	1.73	52.7	4.90	0.71	4.47	0.71
126-18 glass	ICP-MS	2.01	26.1	0.20	0.06	1.77	0.13	2.87	7.85	0.46	1.27	7.3	102.0	71.9	2.00	2.94	1.13	4.21	0.82	5.50	1.22	36.6	3.49	0.50	3.16	0.50
127-05 glass	ICP-MS	23.1	190.3	1.71	0.35	21.8	1.62	15.8	32.0	1.54	3.91	17.4	334.2	135.0	3.27	4.57	1.62	4.82	0.77	4.53	0.84	25.4	2.16	0.29	1.72	0.26
127-05 powder[a]	ICP-MS	17.2	161.5	1.46	0.34	18.5	1.35	13.5	27.3	1.45	3.39	14.9	293.1	105.1	2.86	3.99	1.39	4.07	0.65	3.79	0.74	18.7	1.80	0.24	1.43	0.21
127-11 glass	NA																									
127-11 powder[a]	ICP-MS	16.3	168.7	1.53	0.42	18.4	1.29	13.8	29.5	1.50	3.85	16.5	304.4	109.0	2.90	4.09	1.43	4.20	0.69	3.96	0.76	18.5	1.89	0.26	1.49	0.23
4-1 powder[b]	ICP-MS	27.7	243.5	2.49	0.57	28.0	-	22.2	43.5	1.98	5.13	21.8	406.1	155.4	3.70	5.34	1.77	5.10	0.78	4.41	0.82	24.7	2.04	0.27	1.60	0.24
5–14 glass	ICP-MS	3.58	37.1	0.40	0.10	4.78	0.35	5.89	16.0	0.71	2.53	13.8	155.9	139.1	3.60	5.12	1.89	6.74	1.24	8.06	1.67	51.0	4.69	0.65	4.12	0.66
5–15 glass	ICP-MS	3.46	36.7	0.41	0.12	4.76	0.34	5.72	15.7	0.62	2.49	13.6	156.3	138.6	3.53	5.10	1.88	6.61	1.21	7.92	1.66	51.1	4.62	0.66	4.09	0.62
5–19 glass	ICP-MS	3.52	37.3	0.42	0.12	4.78	0.35	5.82	16.1	0.64	2.52	14.0	157.5	141.1	3.64	5.26	1.86	6.75	1.25	8.07	1.70	51.8	4.69	0.67	4.15	0.64
6–14 glass	ICP-MS	1.16	17.2	0.22	0.05	1.50	0.11	2.48	6.76	0.40	1.09	6.29	103.3	61.4	1.73	2.67	1.09	3.96	0.76	5.04	1.10	34.0	3.11	0.46	2.92	0.46
6–52 glass	ICP-MS	1.46	14.7	0.20	0.06	2.34	0.17	2.42	6.26	0.15	1.01	5.87	175.9	52.1	1.43	2.27	1.03	2.88	0.48	2.81	0.55	16.4	1.36	0.18	1.11	0.16
6–52 powder[a,b]	ICP-MS	1.43	15.1	0.19	0.06	2.30	-	2.36	6.07	0.41	0.98	5.68	171.9	45.7	1.40	2.23	0.99	2.74	0.46	2.75	0.53	13.6	1.36	0.18	1.05	0.16
6–54 glass	ICP-MS	1.39	14.8	0.19	0.05	2.33	0.16	2.41	6.16	0.42	1.00	5.85	171.5	51.1	1.41	2.25	1.01	2.80	0.48	2.80	0.54	16.2	1.38	0.19	1.10	0.16
16-12 glass	ICP-MS	0.77	8.3	0.12	0.03	1.53	0.12	2.65	7.62	0.45	1.26	7.17	126.2	71.5	1.98	2.87	1.13	4.06	0.75	5.02	1.08	32.8	3.03	0.44	2.79	0.44
16-14 glass	ICP-MS	0.50	4.7	0.08	0.03	1.01	0.08	2.17	6.69	0.30	1.14	6.75	123.9	68.3	1.80	2.75	1.10	3.85	0.73	4.90	1.08	32.1	3.01	0.43	2.66	0.42
19-1 glass	ICP-MS	17.0	205.9	2.30	0.55	25.0	1.65	18.9	37.2	1.13	4.48	19.7	240.5	154.4	3.75	5.42	1.82	5.95	1.01	6.18	1.24	38.2	3.33	0.47	2.87	0.44
19-2 glass	ICP-MS	17.6	207.7	2.25	0.48	26.4	1.73	19.4	38.4	1.35	4.59	20.1	247.3	159.5	3.84	5.34	1.85	6.10	1.03	6.25	1.27	38.8	3.42	0.49	2.92	0.45
19-7 glass	ICP-MS	17.5	211.9	2.36	0.57	25.6	1.70	19.4	38.2	1.15	4.57	19.9	245.1	159.9	3.85	5.35	1.84	6.08	1.04	6.37	1.28	39.2	3.42	0.48	2.94	0.45
20-2 glass	ICP-MS	20.2	234.6	2.70	0.63	28.7	1.90	21.4	41.7	1.25	4.93	21.2	270.7	168.4	3.94	5.56	1.81	5.65	0.94	5.60	1.12	34.3	2.98	0.41	2.49	0.38
20-3 glass	ICP-MS	20.1	238.0	2.73	0.66	29.0	1.96	21.9	42.6	1.27	5.12	21.8	274.8	169.1	3.99	5.54	1.87	5.78	0.96	5.64	1.14	34.6	3.03	0.41	2.55	0.39
20-16 glass	ICP-MS	20.2	239.5	2.77	0.65	29.3	1.96	22.0	42.4	1.27	5.04	21.7	271.9	170.8	3.98	5.54	1.84	5.75	0.95	5.72	1.15	34.4	3.01	0.43	2.56	0.38
21-1 glass	ICP-MS	1.07	12.9	0.16	0.04	1.76	0.12	2.18	6.13	0.18	1.01	5.81	88.2	54.3	1.59	2.45	0.97	3.53	0.67	4.55	1.00	30.5	2.79	0.40	2.49	0.39
BHVO-2	ICP-MS	9.2	129	1.27	0.40	17.26	1.23	15.54	35.64	1.61	4.79	22.81	396	176	4.38	6.36	2.20	6.50	1.04	5.77	1.08	32.39	2.67	0.34	1.99	0.29

[a]All samples were measured in this study except for 6–52, 127-05, and 127-11 powders from *Jackson et al*. [2010].
[b]Samples 4-1 and 6-52 were ground in tungsten carbide. Ta from these samples are not included due to possible contamination.

Geochemistry, Geophysics, Geosystems

10.1002/2013GC005061

Table 3. He, Sr, Nd, Hf, and Pb-Isotopic Analyses of Northern Lau Basin and North Fiji Basin Lavas

Sample Name	Phase Analyzed	$^{3}He/^{4}He$ (R/Ra)	Error (2σ)[a]	$[^{4}He]\ 10^{-9}$ cc STP/g	$^{87}Sr/^{86}Sr$[b]	Error (2σ)[a]	$^{87}Sr/^{86}Sr$ Replicate[b]	Error (2σ)[a]	$^{87}Sr/^{86}Sr$ Prev. Publ.[c]	Error (2σ)[a]	$^{143}Nd/^{144}Nd$[c]	Error (2σ)[a]	$^{143}Nd/^{144}Nd$ Replicate	Error (2σ)[a]	$^{143}Nd/^{144}Nd$ Prev. Publ. (renorm.)[d]	Error (2σ)[a]	$^{176}Hf/^{177}Hf$[j]	Error (2σ)[a]	$^{206}Pb/^{204}Pb$[e]	Error (2σ)[a]	$^{207}Pb/^{204}Pb$[e]	Error (2σ)[a]	$^{208}Pb/^{204}Pb$[e]	Error (2σ)[a]
140-1A	glass	1.66	0.06	50	0.703531	10	0.703512	6	0.703461[f]	29	0.513159	5	0.513133	2	0.513079[f]	16	0.283324	7	18.5221	3	15.5302	3	38.3955	11
142-1	glass	8.72	0.26	170	0.703024	36			0.702946[f]	27	0.513102	11	0.513086	10	0.513095[f]	18	0.283321	6	18.4446	21	15.5298	21	38.2873	56
162-1	glass	9.19	0.28	5500	0.702892	14	0.702879	11	0.702819[f]	30	0.513218	16	0.513228	11	0.513199[f]	22	0.283510	8	18.2692	29	15.4896	27	38.0941	51
164-1	glass	2.29	0.38	0.9	0.703668	7	0.703663	14	0.703617[f]	25	0.513069	27			0.513044[f]	17			18.6439	2	15.5473	2	38.4589	7
231-1A	glass	1.48	0.10	5.7					0.703300[f]	27	0.513045	8	0.513037	3	0.513053[f]	18	0.283238	4	18.3777	11	15.5077	10	38.2666	37
13-2	glass	10.02	0.28	300	0.704080	24					0.512905	13	0.512899	8			0.283165	4	18.4060	6	15.5584	5	38.3830	18
13-4	glass	10.45	0.30	210	0.704082	26					0.512896	34	0.512888	4			0.283151	6	18.3928	28	15.5484	22	38.3533	60
126-18	glass	1.75	0.34	1.4	0.703572	12					0.513007	11					0.283224	7	18.4122	18	15.5312	14	38.2498	38
127-05	glass	12.49	0.46	4.4	0.704794	12					0.512772	10							18.6710	18	15.5693	22	38.7674	56
127-05[g]	wr										0.512775								18.6659		15.5773		38.7915	
127-11	glass	14.01	0.44	19	0.704797	16					0.512788	14					0.283007	7	18.6544	5	15.5677	9	38.7577	15
127-11[g]	wr				0.704783						0.512780								18.6748		15.5759		38.7893	
4-1	wr/glass[h]	14.93	0.52	1300	0.705093	30					0.512756	6	0.512748	6			0.283000	4	18.6432	11	15.5732	10	38.8050	31
5–14	glass	5.87	0.34	4.4	0.703385	21			0.703482[i]	49	0.513063	14	0.513068	5	0.513044[i]	35	0.283240	3	18.1588	6	15.4917	5	38.0114	17
5–15	glass	8.32	0.30	480	0.703384	12	0.703376	4	0.703317[i]	29	0.513056	8			0.513111[i]	23			18.1482	21	15.4806	9	37.9833	24
5–19	glass	7.65	0.30	11	0.703394	14					0.513065	14							18.1606	12	15.4875	10	38.0023	46
6–14	glass	9.05	0.36	5.6	0.703761	27					0.512969	11	0.512979	7			0.283217	8	18.3782	15	15.5422	13	38.3463	26
6–52	glass	8.02	0.18	1100					0.703257[i]	25					0.512961[i]	24								
6–52[g]	wr				0.703286						0.513050								18.5691		15.5386		38.4372	
6–54	glass	8.28	0.24	1100	0.703134	9	0.703116	7	0.703434[i]	34	0.513051	9	0.513023	7	0.513011[i]	16	0.283228	5	18.5483	26	15.5268	25	38.3809	74
16-12	glass	9.73	0.22	3600	0.703370	14			0.703407[i]	34	0.513050	26	0.513041	12	0.513054[i]	39	0.283227	7	18.1884	43	15.4824	40	37.9767	89
16-14	glass	9.48	0.28	1700	0.703327	26					0.513010	40	0.513050	14			0.283194	7	18.2159	17	15.4904	16	38.0284	40
19-1	glass	7.62	0.24	31	0.703595	8	0.703585	9			0.512867	6							18.8457	4	15.5607	5	38.8078	23
19-2	glass	8.02	0.22	200	0.703528	25					0.512874	18							18.8436	3	15.5588	1	38.8005	13
19-7	glass	7.46	0.24	16	0.703598	6			0.703589[i]	34	0.512884	4	0.512858	13	0.512842[i]	23	0.283082	5	18.8378	9	15.5586	5	38.7991	12
20-2	glass	7.86	0.24	360	0.703742	9					0.512834	7	0.512818	12			0.283029	5	18.8384	2	15.5787	2	38.9067	7
20-3	glass	7.97	0.24	250	0.703745	2			0.703720[i]	28	0.512827	8	0.512822	6	0.512816[i]	23	0.283029	4	18.8410	3	15.5803	3	38.9113	17
20-16	glass	8.18	0.24	320	0.703738	13			0.703791[i]	35	0.512830	10	0.512821	8	0.512814[i]	24	0.283036	4	18.8378	4	15.5787	2	38.9056	4
21-1	glass	6.05	0.14	5200	0.703846	13					0.512846	11	0.512839	4			0.283083	8	18.3776	53	15.5499	47	38.4052	111

[a]Error is 2σ standard error of the mean, and are absolute (not relative), and are reported as least units cited in the isotope ratio.

[b]Nd-isotopic values are corrected to La Jolla value of 0.511847. Sr-isotopic values are corrected to a NBS 987 value of 0.710240.

[c]Sr isotopes from *Johnson and Sinton* [1990] and *Sinton et al*. [1993] are normalized to Eimer & Amend = 0.7080 which is equivalent to an SRM 987 of approximately 0.70124, so we make no change to their $^{87}Sr/^{86}Sr$ data.

[d]Nd isotopes from *Johnson and Sinton* [1990] and *Sinton et al*. [1993] are normalized to BCR-1 value 0.512640. We ran six BCR-2 standards and measured an average of 0.512625 (normalized to a LaJolla value of 0.511847). BCR-1 and BCR-2 are similar in composition isotopically, and we use the Nd-isotope values of BCR-1 and BCR-2 from *Weis et al*. [2006] to "bridge" the BCR-2 value from this study with the BCR-1 value from the *Sinton et al*. [1993] and *Johnson and Sinton* [1990] studies. The *Sinton et al*. [1993] and *Johnson and Sinton* [1990] $^{143}Nd/^{144}Nd$ values require a 14 ppm reduction for direct comparison with our data, and the $^{143}Nd/^{144}Nd$ ratios from these two publications that are shown in our table have been renormalized (i.e., reduced) accordingly. Discrepancies between our measurements and those of *Johnson and Sinton* [1990] and *Sinton et al*. [1993] are discussed in the supporting information.

[e]Pb-isotopic values corrected to *Todt et al*. [1996] ($^{206}Pb/^{204}Pb = 16.9356$, $^{207}Pb/^{204}Pb = 15.4891$, and $^{208}Pb/^{204}Pb = 36.7006$).

[f]The previously published data from *Johnson and Sinton* [1990].

[g]127-05, 127-11, and 6–52 whole rock data from *Jackson et al*. [2010].

[h]For sample 4-1, helium isotopes were measured on glasses and Sr, Nd, Hf, and Pb-isotopes were measured on whole rock powders.

[i]The previously published data are from *Sinton et al*. [1993].

[j]The unweighted mean $^{176}Hf/^{177}Hf$ ratio of the JMC-475 standard obtained during collection of the present Hf isotope data gave 0.282169 ± 0.000004 (n = 21), which is identical within error to the accepted value of 0.282163 ± 0.000009 [*Blichert-Toft et al*., 1997] for JMC-475. Hence no corrections were applied to the data.

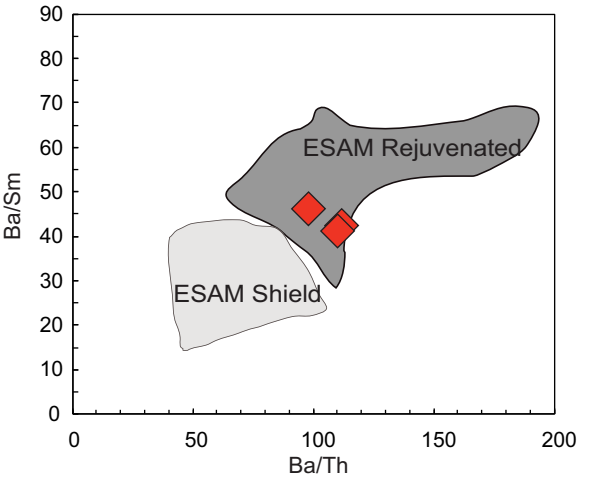

Figure 5. Plot showing Ba/Th versus Ba/Sm for Wallis Island lavas (red symbols) from this study. A similar figure was used by *Jackson et al.* [2010] to resolve shield stage from rejuvenated stage lavas from the Eastern Samoan (ESAM) volcanic province. All trace element data used in this plot, including data used to construct the data fields, were measured by ICP-MS.

3.3. Hf, Pb, Sr, and Nd Isotopes

SPR (dredges 19 and 20) has elevated $^{87}Sr/^{86}Sr$ (up to 0.7037) and low $^{143}Nd/^{144}Nd$ (down to 0.51283) and $^{176}Hf/^{177}Hf$ (down to 0.28303) relative to MORB, which suggest the incorporation of a geochemically enriched component (Figure 6 and Table 2). In plots of various trace element ratios (Ba/Sm, Nb/Zr, La_N/Sm_N, La_N/Lu_N) as a function of $^{143}Nd/^{144}Nd$, SPR lavas consistently plot near or within the field for Samoan Upolu shield lavas (Figure 7). Similarly, the SPR samples plot between MORB and Upolu shield in all isotope spaces that include Nd, Hf, or Pb-isotopic compositions. In each case SPR is shifted slightly away from the Upolu shield field toward depleted mantle along a straight line between the two components. However, in plots that include $^{87}Sr/^{86}Sr$, the SPR samples are shifted closer to MORB and to lower $^{87}Sr/^{86}Sr$, and plot slightly off a simple linear trend connecting Upolu shield and MORB.

The sample taken ~100 km south of SPR (21-1) plots very close to SPR samples in isotopic space, but has slightly higher $^{87}Sr/^{86}Sr$ (0.7038) and lower Pb-isotopic ratios (Figure 6 and Table 2). Moving further to the east, samples 13-2 and 13-4 also plot close to the SPR lavas in isotopic space, but these two samples have even higher $^{87}Sr/^{86}Sr$ (up to 0.7041), but the $^{143}Nd/^{144}Nd$ (as low as 0.51290) and $^{176}Hf/^{177}Hf$ (as low as 0.28315) are shifted to geochemically more depleted compositions.

Futuna Island and Manatu seamount each exhibit a variety of isotopic compositions that range from the compositions found in the SPR region to more depleted compositions that trend toward a MORB-like component. The $^{87}Sr/^{86}Sr$ ratios measured in Futuna Island vary up to 0.7040 [*Jackson et al.*, 2010], while $^{143}Nd/^{144}Nd$ and $^{176}Hf/^{177}Hf$ are as low as 0.51297 and 0.28322, respectively (Table 2). Similarly, samples from Manatu seamount show $^{87}Sr/^{86}Sr$ up to 0.7043, and $^{143}Nd/^{144}Nd$ and $^{176}Hf/^{177}Hf$ of 0.51297 and 0.28322, respectively. Additional lavas from both Manatu seamount and Futuna Island extend to more depleted compositions, with $^{87}Sr/^{86}Sr$ down to 0.7036 and 0.7031, respectively.

Three locations in this study have extremely depleted lavas. All samples from near the Fiji Triple Junction and northeast of Peggy Ridge have $^{143}Nd/^{144}Nd$ (0.51305 and 0.51306) similar to average MORB, but show $^{87}Sr/^{86}Sr$ (0.7033 and 0.7034) that is higher than average MORB. Samples from ~100 km North of Viti Levu, Fiji, likewise are depleted, but show a comparatively wider range in $^{87}Sr/^{86}Sr$ (0.7029–0.7037), $^{143}Nd/^{144}Nd$ (0.51307–0.51322), and $^{176}Hf/^{177}Hf$ (0.28332–0.28351).

Wallis Island lavas sample a mantle source that is broadly similar to that seen in Samoan rejuvenated lavas. The Wallis Island samples plot close to the range of Samoan rejuvenated lavas in all isotope spaces, but are shifted slightly toward MORB (Figure 6). Similarly, various trace element ratios (Ba/Sm, Nb/Zr, La_N/Sm_N, La_N/Lu_N) plotted against $^{143}Nd/^{144}Nd$ show that Wallis Island lavas consistently plot near or within the field of Samoan rejuvenated lavas (Figure 7).

3.4. He Isotope Data

In Figure 8, we present plots of $^{3}He/^{4}He$ versus ^{4}He, $^{87}Sr/^{86}Sr$, $^{143}Nd/^{144}Nd$, and $^{206}Pb/^{204}Pb$ for samples from this study. The highest $^{3}He/^{4}He$ values are from Wallis Island and are up to 15 Ra. A relatively high-$^{3}He/^{4}He$ ratio of 10.45 Ra is recorded in sample 13-4 taken ~300 km north of Viti Levu, and sample 16-12 taken near the North Fiji Basin triple junction has a $^{3}He/^{4}He$ value of 9.7 Ra. All other samples with relatively high helium concentrations exhibit mantle-derived $^{3}He/^{4}He$ between 6.0 and 9.2 Ra.

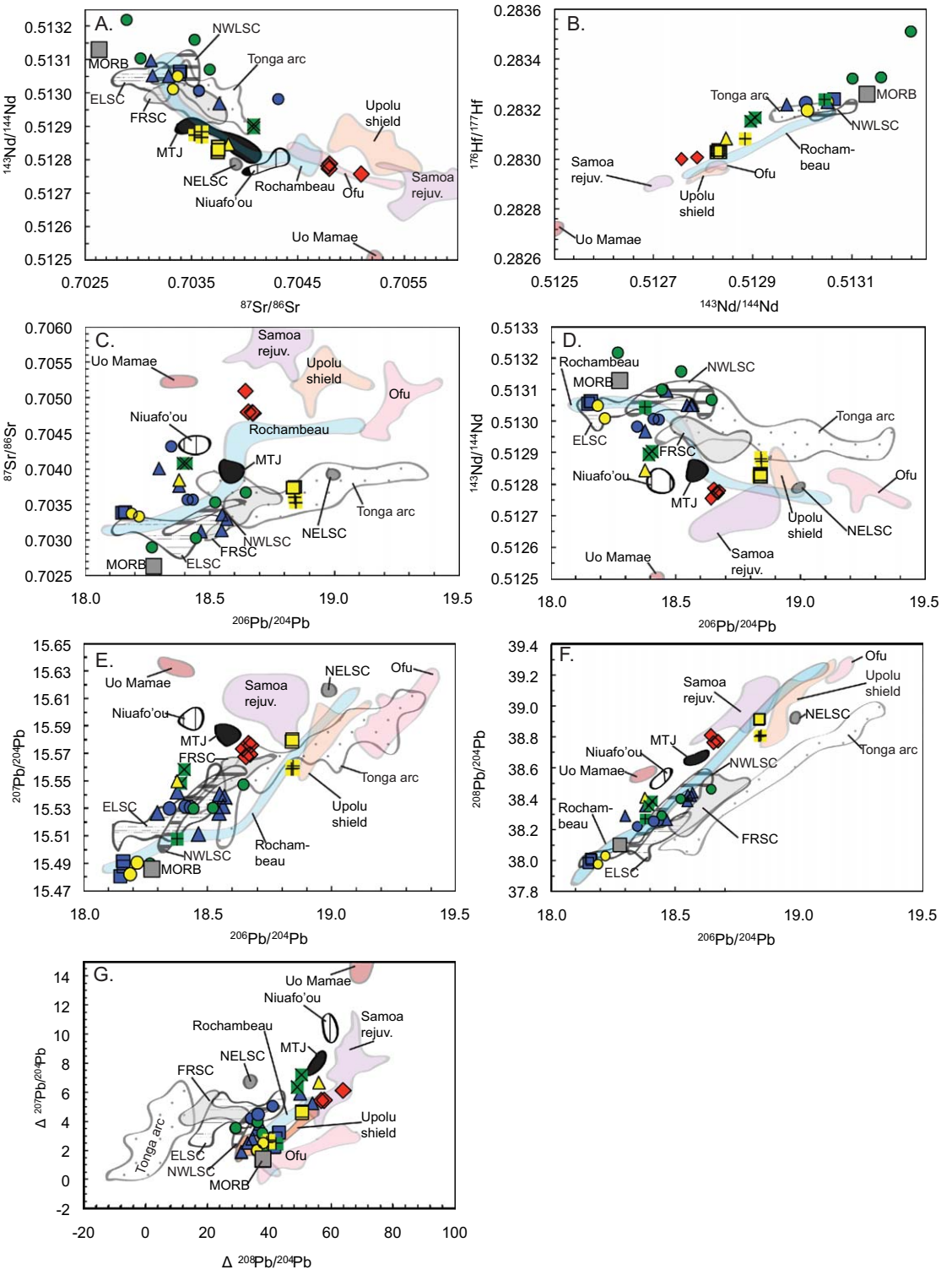

Figure 6. Relationships between Sr, Nd, Hf, and Pb-isotopes in lavas from the northern Lau and North Fiji Basins, Wallis Island and the Samoan hot spot. In addition to new data from this study, previously published values from Wallis, Futuna and Manatu are also shown [*Jackson et al.*, 2010]. Symbols are the same as in Figure 1. Abbreviations: MORB, mid-ocean ridge basalt; NWLSC, Northwest Lau Spreading Center; NELSC, Northeast Lau Spreading Center; FRSC, Fonulai Spreading Center; ELSC, Eastern Lau Spreading Center; MTJ, Mangatolu Triple Junction. The field for Rochambeau includes data from Rochambeau Rift. Lead-isotopic data from Rochambeau Bank are not available. Values for Samoan data fields are from *Wright and White* [1987], *Poreda and Craig* [1992], *Workman et al.* [2004], *Workman and Hart* [2005], *Jackson et al.* [2007a, 2007b, 2010], and *Salters et al.* [2011]. Rochambeau data are from *Lytle et al.* [2012]. Uo Mamae data are from *Pearce et al.* [2007] and *Regelous et al.* [2008]. NELSC data are from *Falloon et al.* [2007] and *Regelous et al.* [2008]. NWLSC data are from *Lytle et al.* [2012]. ELSC data are from *Tian et al.* [2008] and *Escrig et al.* [2009]. FRSC data are from *Escrig et al.* [2012]. Niuafo'ou data are from *Regelous et al.* [2008] and *Tian et al.* [2011]. Mangatolu Triple Junction data are from *Regelous et al.* [2008] and *Tian et al.* [2011]. Tonga arc data are from *Hergt and Woodhead* [2007], *Escrig et al.* [2012], *Turner et al.* [2012], and *Caulfield et al.* [2012]. MORB is from Su and Langmuir [2003].

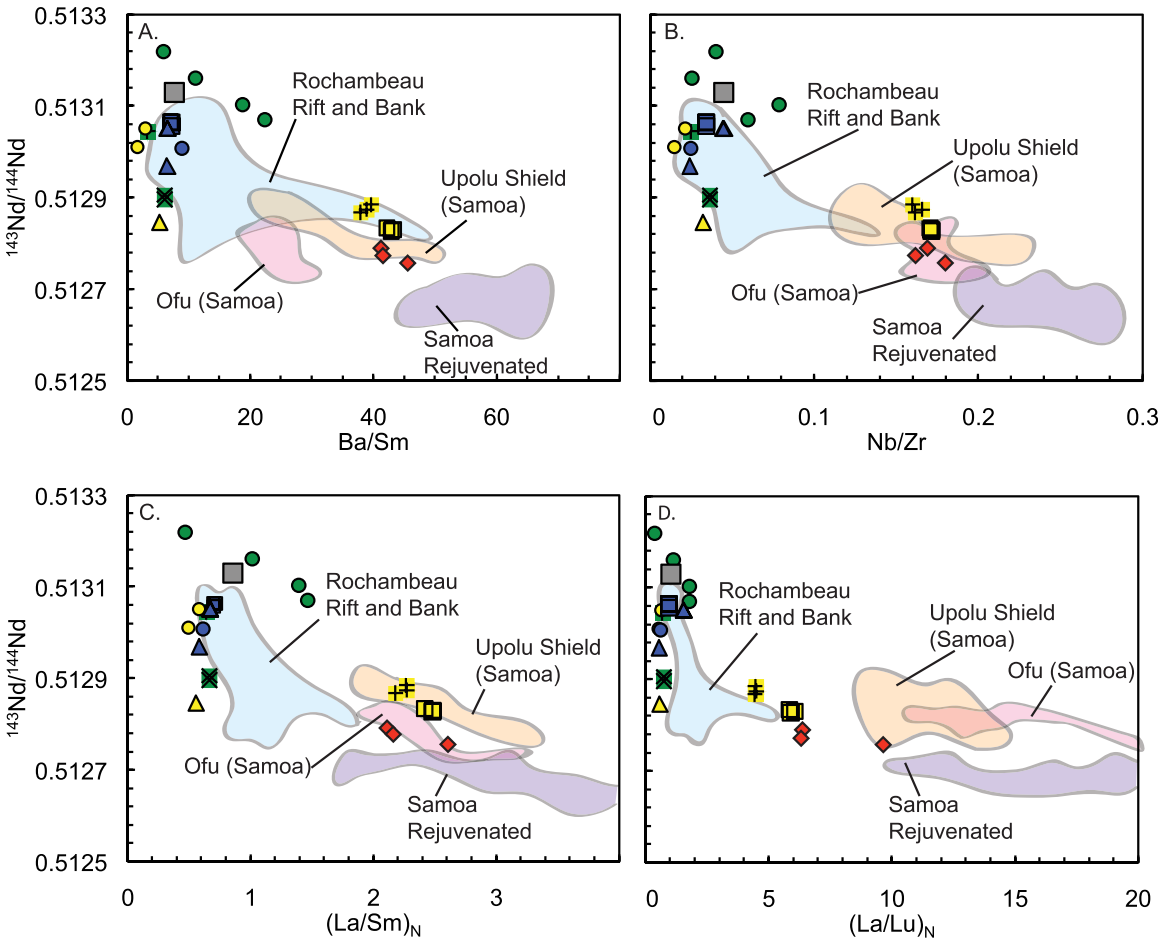

Figure 7. $^{143}Nd/^{144}Nd$ compared to trace element ratios for northern Lau and North Fiji Basins and Samoa. All symbols in this figure are the same as in Figure 1. Average mid-ocean ridge basalt (MORB) is shown as a gray box [*Gale et al.*, 2013]. South Pandora Ridge lavas trend toward the field of Samoan Upolu shield lavas. Wallis Island lavas trend toward the fringes of the Samoan rejuvenated field defined by Savai'i and Upolu rejuvenated lavas. All new trace element data were measured on glasses with the exception of sample 4-1. All trace element data used in this plot, including data used to construct the data fields, were measured by ICP-MS. Rochambeau Rift and Rochambeau Bank are plotted as a single field. Rochambeau data are from *Tian et al.* [2011] and *Lytle et al.* [2012]. Note that *Tian et al.* [2011] has replicate runs of samples from *Volpe et al.* [1988] and *Poreda and Craig* [1992]. Samoan data are from *Hauri and Hart* [1993], *Workman et al.* [2004], and *Jackson et al.* [2007b].

Four samples have $^3He/^4He$ values of <2 Ra. We consider these and other samples with relatively low helium concentrations ($<1 \times 10^{-7}$ ^{4}He cc STP/g) [*Georgen et al.*, 2003] to have experienced incorporation of atmospheric helium or severe posteruptive radiogenic ingrowth. These samples are not plotted in Figures 8b–8d as the measured $^3He/^4He$ does not reflect the mantle composition.

Several salient features are observed in Figure 8. First, Wallis Island has moderately high $^3He/^4He$ with Sr, Nd, and Pb-isotopic compositions that plot near existing data for Samoan rejuvenated lavas on some plots and near Upolu shield lavas on others. Samples taken from ~300 km north of Viti Levu, which exhibit $^3He/^4He$ up to 10.45 Ra, plot between MORB and Wallis lavas in all plots of Figure 8. This suggests the possible involvement of a Samoan component as far as the North Fiji Basin. SPR have lower $^3He/^4He$ (7.5–8.2 Ra) than Samoan Upolu shield lavas, reflecting a shift to a possible MORB-like component with lower $^3He/^4He$. At 6.0 Ra, the sample from south of the SPR (sample 21-1) has the lowest $^3He/^4He$ in the subset of samples with relatively high helium concentrations ($>1 \times 10^{-7}$ ^{4}He cc STP/g). Manatu and Futuna Islands also plot between a MORB-like and a Samoan component, but have MORB-like $^3He/^4He$ of ~8 Ra. In general, all other samples have $^3He/^4He$ ratios and heavy radiogenic isotopic compositions similar to MORB.

In Figure 9, we present a map showing the locations and values of new and previously published $^3He/^4He$ data from Samoa as well as the Lau and North Fiji Basins. The Samoan hot spot has a diversity of isotopic components, and we note that high-$^3He/^4He$ (>20 Ra) lavas are rare in the Samoan hot spot. Nonetheless, $^3He/^4He$ ratios in excess of 20 Ra are identified in the northern Lau Basin.

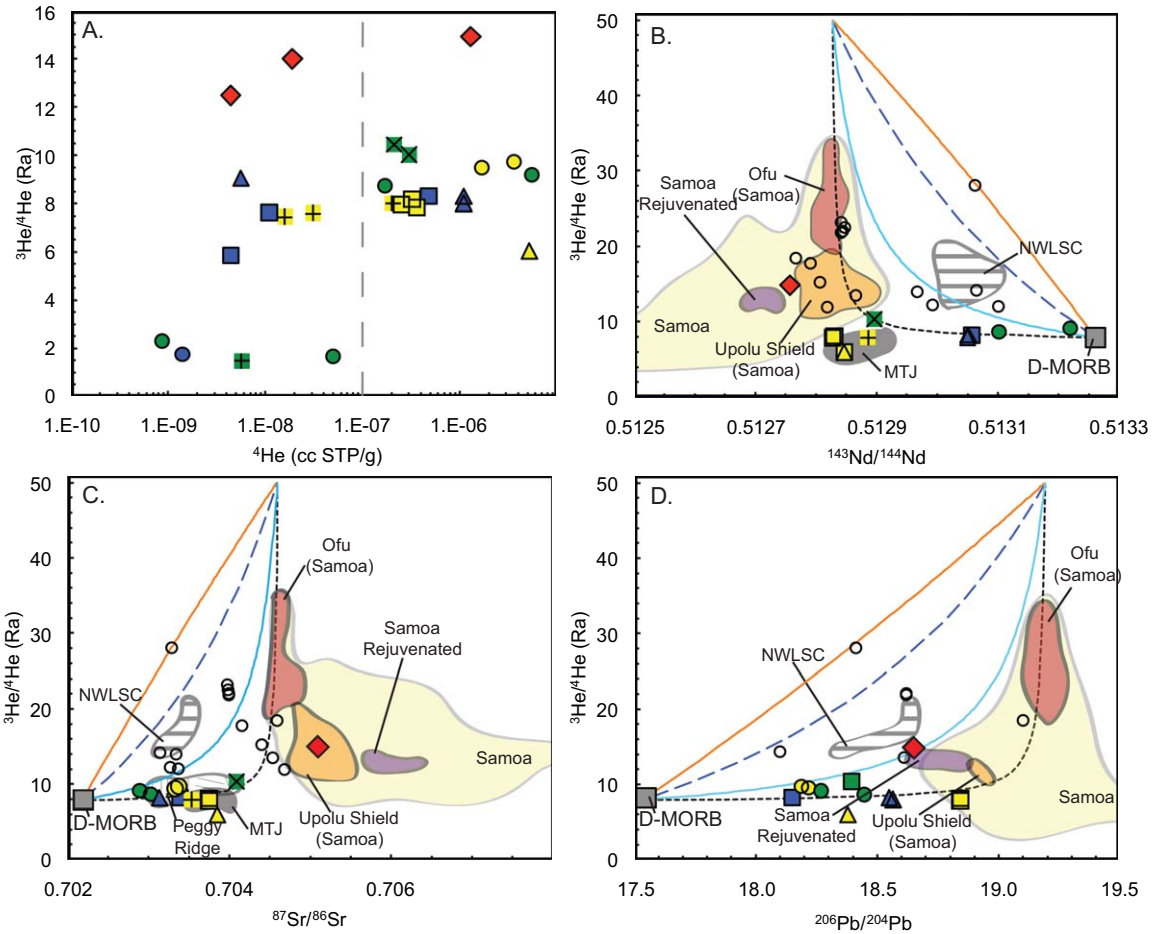

Figure 8. Helium-isotopic data for samples from the northern Lau and North Fiji Basins plotted against their respective gas concentrations, $^{87}Sr/^{86}Sr$, $^{143}Nd/^{144}Nd$, and $^{206}Pb/^{204}Pb$. All new $^3He/^4He$ measurements were made on glasses. Samples with ^4He concentrations $<10^{-7}$ cc STP/g (see vertical dashed line in plot a) are not shown in plots (b) through (d), as many of these samples exhibit evidence for diminished $^3He/^4He$ due to possible post-eruptive radiogenic ingrowth of ^4He or incorporation of atmospheric helium. Symbols in this figure are the same as in Figure 1 with the addition of open circles for previously published Rochambeau Bank and Rift data. Abbreviations: NWLSC, Northwest Lau Spreading Center and MTJ, Mangatolu Triple Junction. The mixing models are described in section 4.2 of the main text and values used in the mixing models are provided in Table 4. In the mixing models, a variably degassed D-MORB (depleted MORB) melt is mixed with a variably degassed high-$^3He/^4He$ melt. The different mixing lines represent variable degassing of the two end-members prior to mixing: the solid orange line assumes that both end-members degassed by the same amount before mixing; the dark blue dashed line assumes that the high-$^3He/^4He$ melt degassed 50% more than the D-MORB melt; the solid light blue line assumes that the high-$^3He/^4He$ melt degassed 90% more than the D-MORB melt; and the small black dashed line assumes that the high-$^3He/^4He$ melt degassed 99% more than the D-MORB melt. Samoan data are from *Workman et al.* [2004] and *Jackson et al.* [2007b, 2010]. Rochambeau Bank and Rift data are from *Volpe et al.* [1988], *Poreda and Craig* [1992], *Lupton et al.* [2009], *Tian et al.* [2011], *Lytle et al.* [2012], and *Hahm et al.* [2012]. Mangatolu Triple Junction data are from *Hilton et al.* [1993], *Tian et al.* [2011], and *Hahm et al.* [2012]. NWLSC data are from *Lupton et al.* [2009] and *Lytle et al.* [2012]. Peggy Ridge data are from *Volpe et al.* [1988], *Tian et al.* [2011], and *Hahm et al.* [2012].

4. Discussion

Systematic spatial variations in geochemical indices (e.g., Sr, Nd, Hf, and Pb-isotope ratios) can be used to assess whether or not a geochemically enriched plume component, such as one associated with Samoa, has intruded into the northern Lau and North Fiji Basins [e.g., *Volpe et al.*, 1988; *Gill and Whelan*, 1989b; *Poreda and Craig*, 1992; *Ewart et al.*, 1998; *Turner and Hawkesworth*, 1998; *Pearce et al.*, 2007]. Geochemical enrichment (e.g., high $^{87}Sr/^{86}Sr$) is clear in lavas from the northern Lau and North Fiji Basins, but diminishes toward the south [e.g., *Pearce et al.*, 2007; *Escrig et al.*, 2009]. The new data offer some important insights into the long-term geochemical connections between Samoa and the Lau and North Fiji Basins.

4.1. How Many High-$^3He/^4He$ Plumes Exist in the Northwest Lau Basin?

Poreda and Craig [1992] found that high-$^3He/^4He$ lavas at Rochambeau Bank in the northwest Lau Basin exhibit increasing $^3He/^4He$ as Sr, Nd, and Pb-isotopic compositions trend from depleted compositions, typical of Lau back arc basins lavas, to more enriched values, typical of the Samoan hot spot. This relationship

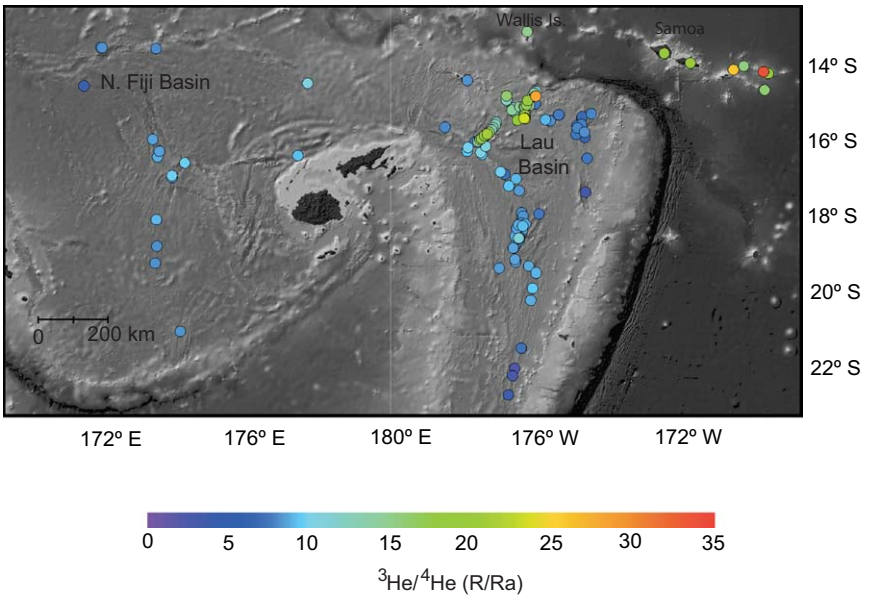

Figure 9. Map of new and previously published $^{3}He/^{4}He$ data from the Lau and North Fiji Basins and Samoa. For Samoan localities, only the highest $^{3}He/^{4}He$ found on each island is shown. Glass samples with ^{4}He concentrations $<10^{-7}$ cc STP/g are not shown. All published data from the Lau and North Fiji Basins are shown, together with Samoan data from *Workman et al*. [2004] and *Jackson et al*. [2007b]. All other data are from this study, *Poreda and Craig* [1992], *Hilton et al*. [1993], *Honda et al*. [1993], *Nishio et al*., [1998], *Lupton et al*. [2009], *Hahm et al*. [2012], and *Lupton et al*. [2012]. Base map was created using GeoMapApp (http://www.geomapapp.org) with topographic and bathymetric data from SRTM_PLUS (*Becker et al*., 2009, v. 5.0)

between $^{3}He/^{4}He$ and the heavy radiogenic isotopes led *Poreda and Craig* [1992] to suggest that a Samoan-plume component has infiltrated the Lau Basin. Subsequent studies have verified the Samoan affinity in lavas from this region [e.g., *Lupton et al*., 2009; *Tian et al*., 2011; *Lupton et al*., 2012; *Hahm et al*., 2012; *Peto et al*., 2013].

However, *Lytle et al*. [2012] found that the lava with the highest $^{3}He/^{4}He$ ratio identified in the Lau Basin—28 Ra [*Lupton et al*., 2009, 2012]—is associated with distinctly non-Samoan Sr, Nd, and Pb-isotopic compositions, and they suggest that such decoupling of $^{3}He/^{4}He$ from the other isotopic systems presents difficulties for the *Poreda and Craig* [1992] model. *Lytle et al*. [2012] showed that the Rochambeau Rift sample with $^{3}He/^{4}He$ of 28 Ra [*Lupton et al*., 2009] has Sr and Nd-isotopic compositions between MORB and Samoan lavas, with $^{87}Sr/^{86}Sr$ of 0.70328 and $^{143}Nd/^{144}Nd$ of 0.51306. By contrast, the Samoan lava with the highest $^{3}He/^{4}He$ has more geochemically enriched $^{87}Sr/^{86}Sr$ (0.70458) and $^{143}Nd/^{144}Nd$ (0.51282) ratios. The geochemical depletion of Rochambeau Rift lavas relative to Samoan lavas with similarly high $^{3}He/^{4}He$ led *Lytle et al*. [2012] to suggest that a Samoan-plume component in the northern Lau Basin may not explain the geochemical composition of high-$^{3}He/^{4}He$ Rochambeau Rift lavas.

We argue that the original single plume model of *Poreda and Craig* [1992] is fully consistent with He-Sr-Nd-Pb-isotopic data from Rochambeau Bank if Samoan-plume melts are variably mixed with ambient depleted mantle melts beneath Rochambeau Bank (Figure 10). To demonstrate the feasibility of this mixing model, we mix two end-member melt compositions, a depleted MORB melt with a high-$^{3}He/^{4}He$ Samoan melt (compositions given in Table 4). The first end-member composition is a depleted MORB (D-MORB) melt with isotopic compositions from *Workman and Hart* [2005] and a trace element composition from *Gale et al*. [2013]. Lavas with geochemically depleted Sr and Nd-isotopic compositions from the northern Lau and North Fiji Basins have been identified in this study (e.g., sample 162-1), implying that the D-MORB end-member is not unrealistic. The helium isotopic composition of the MORB melt is assumed to be 8 Ra [*Graham et al*., 1988], and we adopt the ^{4}He concentration (8.9×10^{-6} cc ^{4}He STP/g) of undegassed MORB primary melt from *Gonnermann and Mukhopadhyay* [2007]. The other end-member melt, derived from the high-$^{3}He/^{4}He$ Samoan-plume component, is assigned the Sr, Nd, and Pb-isotopic compositions of the highest $^{3}He/^{4}He$ Samoan lava (sample Ofu-04–06, with 33.8 Ra, from *Jackson et al*. [2007b]); the corresponding

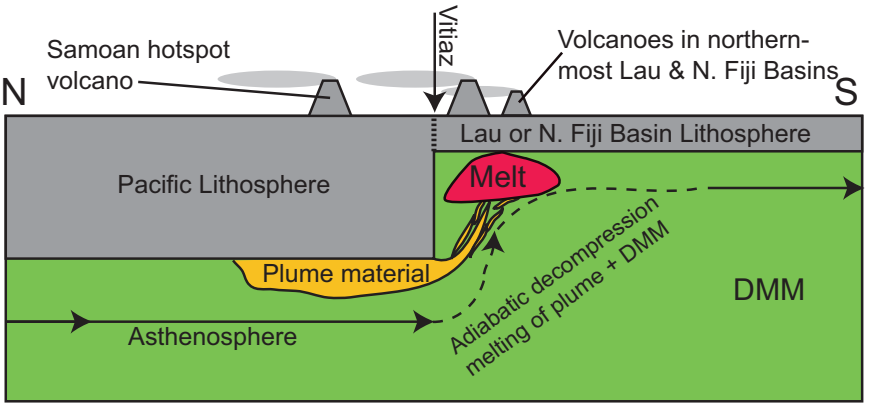

Figure 10. Cartoon of a north-south cross section from the 100 Ma Pacific lithosphere to the 5 Ma lithosphere in the northern Lau and North Fiji Basins. The figure shows the "step" in lithospheric thickness going to the south. Samoan mantle transiting from under the thick Pacific lithosphere to the thin lithosphere of the northern Lau and North Fiji Basins undergoes adiabatic decompression melting as it upwells. Together with the southward flowing plume material, a component of ambient depleted mantle likely melts during this process, thereby contributing a component of depleted mantle (MORB) melt to the final erupted lavas. This may explain the isotopic shift of the lavas in northern Lau Basin lavas (e.g., Rochambeau Bank) away from Samoa and toward a depleted mantle component.

Sr, Nd, and Pb concentrations are inferred from liquid lines of descent for lavas from the Samoan high-^{3}He/^{4}He island of Ofu, where the primary melt is assumed to have 15 wt. % MgO. The ^{3}He/^{4}He ratio of the Samoan-plume melt is assumed to be 50 Ra, the highest mantle ^{3}He/^{4}He ratio measured in a terrestrial, mantle-derived lava [*Stuart et al*., 2003]. This is higher than observed for Samoan lavas, but a higher ^{3}He/^{4}He (50 Ra) in the Samoan mantle cannot be excluded and is not an unreasonable value for the purposes of this model. The ^{4}He concentration of the Samoan-plume melt (2.4×10^{-5} cc ^{4}He STP/g) is the same as the OIB end-member from *Gonnermann and Mukhopadhyay* [2007]. When the two undegassed end-member melts are mixed, the mixing line passes through the highest ^{3}He/^{4}He lava from Rochambeau Rift (28 Ra) at Sr, Nd, and Pb-isotopic compositions intermediate between MORB and the highest ^{3}He/^{4}He Samoan lavas (Figure 8). This mixing model also works if the MORB and Samoan high-^{3}He/^{4}He melts are degassed by the same percentage prior to mixing. Alternative mixing models are also shown which assume that the plume melts degas more than the MORB melts, an assumption supported by recent modeling [*Gonnermann and Mukhopadhyay*, 2007]. These additional mixing models span much of the range in isotopic compositions identified in the northern Lau Basin lavas (Figure 8). In summary, variably degassed mixtures of MORB and high-^{3}He/^{4}He Samoan-plume melts can generate the high-^{3}He/^{4}He signatures and the non-Samoan Sr, Nd, and Pb isotopic compositions observed in Lau Basin lavas.

4.2. Long-Term Influence of Samoan-Plume Material on the Northwest Lau and North Fiji Basins: Evidence From South Pandora Ridge

The influx of the Samoan-plume material may be a long-term process that has operated for the past 4–5 Ma in the northern Lau and North Fiji Basins. *Hart et al*. [2004] suggested that the portion of the Vitiaz Lineament east of 180° resulted from the Pacific plate tearing as the northern terminus of the Tonga Trench migrated west (Figure 1). *Hart et al*. [2004] place the northern terminus of the trench just to the south of

Table 4. Parameters Used in Mixing Model[a]

	MORB End-Member	Source	High-^{3}He/^{4}He End-Member	Source
He (cm^{3} STP/g)	8.90×10^{-6} cm^{3} STP/g	*Gonnermann and Mukhopadhyay* [2007]	2.40×10^{-5} cm^{3} STP/g	*Gonnermann and Mukhopadhyay* [2007]
Sr (ppm)	129 ppm	*Gale et al*. [2013]	320 ppm	*Jackson et al*. [2007b]
Nd (ppm)	12.0 ppm	*Gale et al*. [2013]	29 ppm	*Jackson et al*. [2007b]
Pb (ppm)	0.57 ppm	*Gale et al*. [2013]	1.8 ppm	*Jackson et al*. [2007b]
^{3}He/^{4}He (Ra)	8	*Graham et al*. [1988]	50	*Stuart et al*. [2003]
^{87}Sr/^{86}Sr	0.702190	D-MORB [*Workman and Hart* 2005]	0.704584	*Jackson et al*. [2007b]
^{143}Nd/^{144}Nd	0.513260	D-MORB[*Workman and Hart* 2005]	0.512827	*Jackson et al*. [2007b]
^{206}Pb/^{204}Pb	17.537	D-MORB[*Workman and Hart* 2005]	19.189	*Jackson et al*. [2007b]

[a]Sr, Nd, and Pb concentrations for the high-^{3}He/^{4}He end-member are inferred from liquid lines of descent for lavas from the Samoan high-^{3}He/^{4}He island of Ofu, where the primary melt is assumed to have 15 wt. %.

Rotuma Island at 4 Ma. Dredges 19 and 20 along SPR are no further west of Rotuma than Rochambeau is west of the northern terminus of the Tonga Trench. Thus, we suggest that, at 4 Ma, Samoan mantle material was advected around the paleo-Tonga slab to the west of Rotuma (under the present-day location of SPR) in the same way toroidal flow around the present-day Tonga slab advects material beneath Rochambeau (Figures 2 and 10). We argue that the moderate isotopic enrichment in SPR lavas owes its existence to the incorporation of a Samoan mantle component into the mantle beneath SPR. Because the trace of the known Samoan hot spot extends as far west as Alexa Bank (*Hart et al*., 2004)—just to the north of the North Fiji Basin—it is possible that Samoan mantle material has been available (perhaps as a "keel" attached to the base of the Pacific lithosphere beneath the trace of the Samoan hot spot) for southward advection into the region now occupied by SPR. However, we cannot exclude the possibility that Samoan mantle material was advected to the south of the Vitiaz Lineament more recently due to broad southward mantle flow in the region [*Pearce et al*., 2007] over time, perhaps owing to flattening and lateral spreading of the Samoan underplated keel that would push it south of the Vitiaz Lineament and into the North Fiji Basin.

One further possibility for the presence of a Samoan-plume component in the northern Lau Basin is that the Lau and North Fiji Basins may have been impregnated with small amounts of Samoan-plume melt over a longer period of geologic time. Modeling in N. J. Katsiaficas, P. S. Hall, and M. G. Jackson, Modeling flow of Samoan-plume mantle into the northern Lau Basin, submitted to *Physics of the Earth Planetary Interiors* (2013) has shown that decompression melting at the boundary between thick and thin lithosphere, in the vicinity of the Vitiaz Lineament, is dynamically feasible (Figures 1, 2, and 10). Southward flowing Samoan mantle would pass from beneath older, thicker (100 Ma) Pacific lithosphere and upwell beneath younger, thinner ($<$5 Ma) lithosphere in the northern Lau and North Fiji Basins, generating decompression melts [*Pearce et al*., 2007; *Regelous et al*., 2008; Katsiaficas et al., submitted manuscript, 2013]. During a later event of tectonic extension, such as that which may be occurring at SPR [*Sinton et al*., 1993], the depleted mantle enriched with Samoan-plume melt could be melted to generate the compositions that we observe. Such a scenario may also explain why some of the young lavas in the northern Lau and North Fiji Basins geochemically resemble mixtures between depleted mantle and OIB mantle [e.g., *Johnson and Sinton*, 1990; *Poreda and Craig*, 1992; *Sinton et al*., 1993; *Jackson et al*., 2010]: adiabatic upwelling of plume material in a back-arc basin dominated by depleted mantle would result in melting of depleted mantle together with Samoan-plume material. Melts resulting from both Upolu-like mantle and depleted mantle may mix to form SPR lavas, and explain the slightly depleted trace elements (Figure 4) and isotopic compositions (Figures 6 and 8), of SPR lavas relative to Upolu lavas. Such a model may also explain the slightly less enriched lava dredged $\sim$100 km south of SPR (sample 21-1). This sample is more MORB-like than SPR lavas, but the enrichment in $^{87}Sr/^{86}Sr$ (up to 0.7038) requires an enriched component similar to the Upolu-like component inferred for SPR lavas (Figure 6).

4.3. Are Manatu and Futuna Volcanoes the Result of Melted Mixtures of Samoan Plume and Ambient Depleted Mantle?

Futuna Island and Manatu Seamount are located approximately midway between the present-day northern terminus of the Tonga trench and SPR. Like Rochambeau lavas, Manatu and Futuna lavas have isotopic compositions that plot between MORB and the field of Samoan lavas in multiisotope space (Figure 6). Therefore, *Jackson et al*. [2010] suggested that, like SPR in this study, Futuna and Manatu were fed by mixtures of adiabatic melts of upwelling Samoan mantle material and ambient depleted mantle that transited southward beneath the Vitiaz Lineament into the northwest Lau Basin. However, the Futuna samples have low $^{3}He/^{4}He$ (8–9 Ra) (the Manatu sample was compromised by posteruptive radiogenic ^{4}He ingrowth). However, low-$^{3}He/^{4}He$ ratios of 8 Ra are not uncommon in the Samoan hot spot [*Workman et al*., 2004; *Jackson et al*., 2010]. Therefore, like at SPR, we favor the incorporation of a low-$^{3}He/^{4}He$ Samoan component into the mantle beneath Manatu and Futuna that, together with ambient depleted mantle, was melted to generate lavas for these two volcanoes.

The new trace element data on fresh glasses from Manatu and Futuna reveal relatively smooth patterns that do not suggest an arc-related signature, and the "jagged" nature of the spidergrams of the whole rock samples from *Jackson et al*. [2010] are likely compromised by submarine weathering, particularly for K, U, and Rb. The lack of any clear arc signature in Manatu and Futuna lavas from this study is consistent with the younger eruption ages ($<$5 Ma) [*Duncan*, 1985; *Koppers et al*., 2011] that greatly postdate the end of

subduction along the Vitiaz Lineament at 12 Ma. Previous work identified possible arc-related volcanism in the early history of Futuna, but Futuna transitions to OIB-type volcanism later in its history [*Grzesczyk et al*., 1991]. However, we find that a plot of Ba/Nb versus $^{87}Sr/^{86}Sr$ (Figure 11) shows no arc influence in the suite of Manatu and Futuna lavas presented here, and the Futuna lavas in our sample suite must sample the later OIB state of volcanism on Futuna. Therefore, we prefer to explain the origin of these near-Vitiaz Lineament volcanoes by adiabatic upwelling of Samoan mantle material flowing southward into the northwest Lau Basin. Such a model can be extended to explain the origin of other geochemically enriched localities in the region that have isotopic compositions between depleted mantle and Samoan-plume mantle, such as samples 13-2 and 13-4 from ~300 km north of Viti Levu, Fiji ($^{87}Sr/^{86}Sr = 0.7041$; Figure 6).

4.4. Moderately High $^{3}He/^{4}He$ at Wallis: Further Evidence for a Samoan Heritage

Located immediately to the north of the Vitiaz Lineament and ~400 km to the West of Savai'i, Wallis Island shows evidence for volcanism that may be linked to the tectonic processes operating in the region. To understand the possible origin of recent volcanism on Wallis Island, we draw on knowledge of the Samoan Island of Savai'i, which has been completely resurfaced by large volumes of rejuvenated volcanism. The location of Savai'i near the northern terminus of the Tonga Trench led previous authors to suggest a link between the stresses associated with tearing the Pacific plate at the northern terminus and the large volumes of rejuvenated volcanism [*Hawkins and Natland*, 1975; *Natland*, 1980; *Natland and Turner*, 1985; *Hart et al*., 2004; *Konter and Jackson*, 2012]. Like Savai'i, Wallis Island is located at the northern terminus of the Tonga Trench, and a tectonic origin for the recent volcanism on Wallis has been proposed [*Price and Kroenke*, 1991; *Hart et al*., 2004; *Jackson et al*., 2010].

Like Savai'i rejuvenated lavas [*Konter and Jackson*, 2012], the lavas on Wallis are quite young (0.8–0.08 Ma) [*Duncan*, 1985; *Price and Kroenke*, 1991]. The geochemistry of Wallis Island lavas shows similarities with Samoan rejuvenated lavas. In multiisotope space (Figures 6 and 8), Wallis Island lavas trend into, or plot very close to, the field of Samoan rejuvenated lavas. Additionally, the elevated $^{3}He/^{4}He$ ratios (up to 15 Ra) observed for Wallis Island are similar to slightly elevated $^{3}He/^{4}He$ of Samoan rejuvenated lavas from *Workman et al*. [2004]. Finally, trace element ratios (Figure 5) show that Wallis lavas are enriched in Ba relative to other trace elements, a signature that is shared with Samoan rejuvenated lavas and spidergrams of Wallis Island lavas (Figure 4) show broad similarities with Samoan rejuvenated lavas.

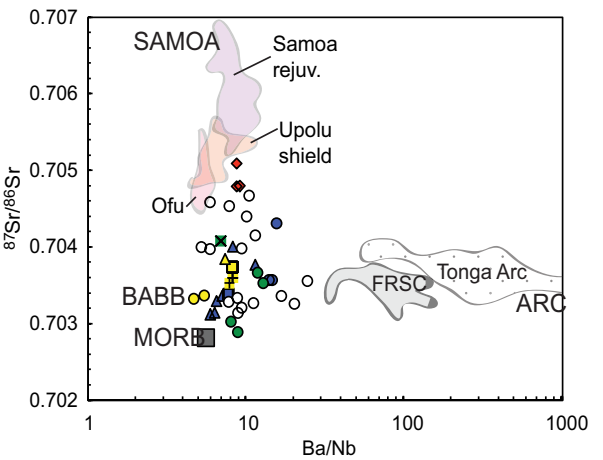

Figure 11. Plot showing Ba/Nb versus $^{87}Sr/^{86}Sr$ for new data and previously published data from Rochambeau Bank and Rift, Samoa (Samoa rejuvenated, Upolu Shield, and Ofu), Fonulai Rift and Spreading Center, the Tonga Arc, as well as average MORB. Symbols are the same as in Figure 1 with the addition of open circles for previously published Rochambeau Bank and Rift data. New samples from this study appear to be uninfluenced by the arc, though three or four of the Rochambeau samples have slightly high Ba/Nb and may host an arc component. Values for MORB are taken from *Gale et al*. [2013]. Rochambeau Bank and Rift data are from *Poreda and Craig* [1992], *Lytle et al*. [2012], and *Tian et al*. [2012]. Fonulai Rift and Spreading center data are from *Escrig et al*. [2012]. Tonga Arc data are from *Ewart et al*. [1998], *Hergt and Woodhead* [2007], *Pearce et al*. [2007], *Escrig et al*. [2012], *Turner et al*. [2012] and *Caulfield et al*. [2012]. Samoan data are from *Wright and White* [1987], *Poreda and Craig* [1992], *Workman et al*. [2004], *Workman and Hart* [2005], and *Jackson et al*. [2007a, 2007b, 2010].

The new geochemical data suggest a common tectonic link for magma generation at both Savai'i and Wallis islands, and that the lavas on both islands share a common genetic ancestry with the Samoan hot spot. If the volcanic evolution of Wallis is similar to Savai'i [*Jackson et al*., 2007a; *Koppers et al*., 2008], an older shield stage may exist in the deep stratigraphy of Wallis Island that has not yet been sampled. While two deep dredges (KK820316 dredge 4 and ALIA 2005 dredge 127) on the western flanks of Wallis Island failed to reveal a deeper shield stage this could be due to sampling: deep dredges of Savai'i have yielded both rejuvenated (ALIA 2005 dredge 116 in *Jackson et al.* [2010]) and shield-stage lavas (ALIA 2005 dredges 114 and 115. Therefore, if the young

volcanism on Wallis relates to a rejuvenated stage, additional sampling on Wallis Island could reveal an older shield stage.

5. Conclusions

Based on our new isotopic data from the northern Lau and North Fiji Basins, we conclude that high-^{3}He/^{4}He lavas (up to 28 Ra) [*Lupton et al*., 2009] along Rochambeau Rift can be explained by mixing melts of a high-^{3}He/^{4}He Samoan-plume component (with an assumed value of 50 Ra) with MORB melts. This model explains why the high-^{3}He/^{4}He lavas in the Rochambeau region also have Sr, Nd, and Pb-isotopic compositions displaced toward MORB values. We argue that southward flow of Samoan-plume mantle into the northern Lau Basin explains the presence of a Samoan-plume signature in volcanoes (e.g., Rochambeau) in the region, and the flow is likely toroidal, driven by roll-back of the Tongan slab. Mantle undergoes decompression melting as it flows south from underneath the thick, old Pacific lithosphere, across the Vitiaz Lineament, and rises adiabatically to the base of the thin, young lithosphere in the Lau Basin. During adiabatic upwelling, ambient depleted upper mantle is likely to melt along with Samoan-plume mantle. This mechanism can explain why volcanic samples from the northern Lau Basin are shifted in isotopic space away from Samoan lava compositions and toward depleted mantle compositions.

We also find that the isotopic compositions of SPR lavas in the North Fiji Basin are consistent with the incorporation of a Samoan-plume component like that found at Upolu Island. At 4 Ma, plate reconstruction places the Tonga Trench near the present-day location of Rotuma, which anchors the northeastern terminus of the SPR. We therefore suggest that, at 4 Ma, Samoan mantle material was advected around the paleo-Tonga slab to the west of the present-day location of Rotuma (and under the present-day location of SPR) in the same way that toroidal flow around the present-day Tonga slab advects Samoan material in the northern Lau Basin beneath Rochambeau. During this southward flow, Samoan mantle material and ambient depleted mantle underwent adiabatic decompression during southward transit beneath the Vitiaz Lineament and into the North Fiji Basin. As well as explaining enrichment in the Rochambeau region (^{87}Sr/^{86}Sr up to 0.7047) and SPR (^{87}Sr/^{86}Sr up to 0.7037), this simple model explains the geochemical enrichment throughout the northern region of the northern Lau and North Fiji Basins, including Manatu seamount (^{87}Sr/^{86}Sr up to 0.7043), Futuna Island (^{87}Sr/^{86}Sr up to 0.7038), samples dredged ~300 km north of Viti Levu, Fiji (^{87}Sr/^{86}Sr up to 0.7041), and a dredge ~100 km south of SPR (^{87}Sr/^{86}Sr = 0.7038).

Finally we show that recent rejuvenated volcanism on Wallis Island may be associated with stresses caused by tearing the Pacific plate at the northern terminus of the Tonga Trench. Trace elements and isotopic compositions in Wallis Island lavas exhibit strong affinities to the rejuvenated lavas of several Samoan islands. The new geochemical data, including moderately high ^{3}He/^{4}He (up to 15 Ra), supports the hypothesis that Wallis Island has a Samoan pedigree.

Acknowledgments

We thank Marcel Regelous and Jim Natland for discussion, and Stephane Escrig for analytical assistance. We thank John Lassiter, Bill White, and Anthony Koppers for their detailed and thoughtful reviews and Thorsten Becker for editorial handling. M.G.J. acknowledges support from NSF grants OCE-1061134, OCE-1153894, and EAR-1145202 and J.B.T. acknowledges support from the French Agence Nationale de la Recherche (grant ANR-10-BLANC-0603 M&Ms—Mantle Melting—Measurements, Models, Mechanisms).

References

Auzende, J.-M., B. Pelletier and J.-P. Eissen (1995), The North Fiji Basin: Geology, structure and geodynamic evolution, in *Backarc Basins: Tectonics and Magmatism*, edited by B. Taylor, pp. 139–175, Plenum, New York.

Becker, J. J., et al. (2009), Global bathymetry and elevation data at 30 arc seconds resolution: SRTM30_PLUS. *Marine Geodesy*, *32*(4), 355–371.

Begg, G., and D. R. Gray (2002), Arc dynamics and tectonic history of Fiji based on stress and kinematic analysis of dikes and faults of the Tavua Volcano, Viti Levu Island, Fiji, *Tectonics*, *21*(4), 5-1–5–14.

Bevis, M., et al. (1995), Geodetic observations of very rapid convergence and back-arc extension at the Tonga arc, *Nature*, *374*(6519), 249–251.

Blichert-Toft, J., C. Chauvel, and F. Albarède (1997), Separation of Hf and Lu for high-precision isotope analysis of rock samples by magnetic sector-multiple collector ICP-MS, *Contrib. Mineral. Petrol.*, *127*(3), 248–260.

Brocher, T. M. (1985), On the formation of the Vitiaz trench lineament and North Fiji basin, in *Investigations of the Northern Melanesian Borderland, Circum-Pac. Counc. for Energy and Miner. Resour. Earth Sci. Ser.*, vol. 3, Earth Science Series, pp. 13–33, ed. Brocher T.M., Circum-Pac. Counc. for Energy and Miner. Resour., Houston, Tex.

Calmant, S., B. Pelletier, P. Lebellegard, M. Bevis, F. W. Taylor, and D. A. Phillips (2003), New insights on the tectonics along the New Hebrides subduction zone based on GPS results, *J. Geophys. Res.*, *108*(B6), 2319, doi:10.1029/2001JB000644.

Caulfield, J., S. Turner, I. Smith, L. B. Cooper, and G. A. Jenner (2012), Magma evolution in the primitive, intra-oceanic Tonga Arc: Petrogenesis of basaltic andesites at Tofua volcano, *J. Petrol.*, *53*(6), 1197–1230.

Crawford, A. J., S. Meffre, and P. A. Symonds (2003), 120 to 0 Ma tectonic evolution of the southwest Pacific and analogous geological evolution of the 600 to 220 Ma Tasman Fold Belt System, *Geol. Soc. Am. Spec. Pap.*, *372*, 383–404.

Duncan, R. A. (1985), Radiometric ages from volcanic rocks along the New Hebrides-Samoa lineament, in *Investigations of the Northern Melanesian Borderland, Circum-Pac. Counc. for Energy and Miner. Resour. Earth Sci. Ser.*, vol. 3, Earth Science Series, pp. 67–75, edited by T. M. Brocher, Circum-Pac. Counc. for Energy and Miner. Resour., Houston, Tex.

Escrig, S., A. Bézos, S. L. Goldstein, C. H. Langmuir, and P. J. Michael (2009), Mantle source variations beneath the Eastern Lau Spreading Center and the nature of subduction components in the Lau basin-Tonga arc system, *Geochem. Geophys. Geosyst.*, *10*, Q04014, doi: 10.1029/2008GC002281.

Escrig, S., A. Bézos, C. H. Langmuir, P. J. Michael, and R. J. Arculus (2012), Characterizing the effect of mantle source, subduction input and melting in the Fonualei Spreading Center, Lau Basin: Constraints on the origin of the boninitic signature of the back-arc lavas, *Geochem. Geophys. Geosyst.*, *13*, Q10008, doi:10.1029/2012GC004130.

Ewart, A., K. D. Collerson, M. Regelous, J. I. Wendt, and Y. Niu (1998), Geochemical evolution within the Tonga-Kermadec-Lau arc-back-arc systems: The role of varying mantle wedge composition in space and time, *J. Petrol.*, *39*(3), 331–368.

Falloon, T. J., et al. (2007), Multiple mantle plume components involved in the petrogenesis of subduction-related lavas from the northern termination of the Tonga Arc and northern Lau Basin: Evidence from the geochemistry of arc and backarc submarine volcanics, *Geochem. Geophys. Geosyst.*, *8*, Q09003, doi:10.1029/2007GC001619.

Farley, K. A., J. Natland, and H. Craig (1992), Binary mixing of enriched and undegassed (primitive?) mantle components (He, Sr, Nd, Pb) in Samoan lavas, *Earth Planet. Sci. Lett.*, *111*(1), 183–199.

Gale, A., C. A. Dalton, C. H. Langmuir, Y. Su, and J.-G. Schilling (2013), The mean composition of ocean ridge basalts, *Geochem. Geophys. Geosyst.*, *14*, 489–518, doi:10.1029/2012GC004334.

Georgen, J. E., M. D. Kurz, H. J. B. Dick, and J. Lin (2003), Low $^{3}He/^{4}He$ ratios in basalt glasses from the western Southwest Indian Ridge (10°–24°E), *Earth Planet. Sci. Lett.*, *206*(3), 509–528.

Giardini, D., and J. H. Woodhouse (1986), Horizontal shear flow in the mantle beneath the Tonga arc, *Nature*, *319*, 551–555.

Gill, J. B. (1984), Sr-Pb-Nd isotopic evidence that both MORB and OIB sources contribute to oceanic island arc magmas in Fiji, *Earth Planet. Sci. Lett.*, *68*(3), 443–458.

Gill, J. B., and P. M. Whelan (1989a), Early rifting of an oceanic island arc (Fiji) produced shoshonitic to tholeiitic basalts, *J. Geophys. Res.*, *94*(B4), 4561–4578.

Gill, J. B., and P. M. Whelan (1989b), Postsubduction ocean island alkali basalts in Fiji, *J. Geophys. Res.*, *94*(B4), 4579–4588.

Gonnermann, H. M., and S. Mukhopadhyay (2007), Non-equilibrium degassing and a primordial source for helium in ocean-island volcanism, *Nature*, *449*(7165), 1037–1040.

Govers, R., and M. J. R. Wortel (2005), Lithosphere tearing at STEP faults: Response to edges of subduction zones, *Earth Planet. Sci. Lett.*, *236*(1), 505–523.

Grzesczyk, A., C. Lefevre, M. Monzier, J.-P. Eissen, J. Dupont, and P. Maillet (1991), Evidence for an upper Pliocene transitional volcanism on Futuna and Alofi islands (South-West Pacific): New contributions to the North Tonga geodynamic evolution, *C. R. Acad. Sci., Ser. II*, *312*(7), 713–720.

Hahm, D., D. R. Hilton, P. R. Castillo, J. W. Hawkins, B. B. Hanan, and E. H. Hauri (2012), An overview of the volatile systematics of the Lau Basin—Resolving the effects of source variation, magmatic degassing and crustal contamination, *Geochim. Cosmochim. Acta*, *85*, 88–113.

Hart, S., et al. (2000), Vailulu'u undersea volcano: The new Samoa, *Geochem. Geophys. Geosyst.*, *1*(12), 1056, doi: 10.1029/2000GC000108.

Hart, S., M. Coetzee, R. Workman, J. Blusztajn, K. Johnson, J. Sinton, B. Steinberger, and J. Hawkins (2004), Genesis of the Western Samoa seamount province: Age, geochemical fingerprint and tectonics, *Earth Planet. Sci. Lett.*, *227*(1), 37–56.

Hauri, E. K., and S. R. Hart (1993), ReOs isotope systematics of HIMU and EMII oceanic island basalts from the south Pacific Ocean, *Earth Planet. Sci. Lett.*, *114*(2), 353–371.

Hawkins, J. W., and J. Natland (1975), Nephelinites and basanites of the Samoan linear volcanic chain: Their possible tectonic significance, *Earth Planet. Sci. Lett.*, *24*(3), 427–439.

Hergt, J., and J. Woodhead (2007), A critical evaluation of recent models for Lau-Tonga arc-backarc basin magmatic evolution, *Chem. Geol.*, *245*(1), 9–44.

Hilton, D. R., K. Hammerschmidt, G. Loock, and H. Friedrichsen (1993), Helium and argon isotope systematics of the central Lau Basin and Valu Fa Ridge: Evidence of crust/mantle interactions in a back-arc basin, *Geochim. Cosmochim. Acta*, *57*(12), 2819–2841.

Hofmann, A. W. (1997), Mantle geochemistry: The message from oceanic volcanism, *Nature*, *385*(6613), 219–229.

Honda, M., D. B. Patterson, I. McDougall, and T. J. Falloon (1993), Noble gases in submarine pillow basalt glasses from the Lau Basin: Detection of a solar component in backarc basin basalts, *Earth Planet. Sci. Lett.*, *120*(3), 135–148.

Jackson, M. G., S. R. Hart, N. Shimizu, and J. S. Blusztajn (2009), The $^{87}Sr/^{86}Sr$ and $^{143}Nd/^{144}Nd$ disequilibrium between Polynesian hot spot lavas and the clinopyroxenes they host: Evidence complementing isotopic disequilibrium in melt inclusions, *Geochem. Geophys. Geosyst.*, *10*, Q03006, doi:10.1029/2008GC002324.

Jackson, M. G., S. R. Hart, A. A. P. Koppers, H. Staudigel, J. Konter, J. Blusztajn, M. Kurz, and J. A. Russell (2007a), The return of subducted continental crust in Samoan lavas, *Nature*, *448*(7154), 684–687.

Jackson, M. G., M. Kurz, S. Hart, and R. K. Workman (2007b), New Samoan lavas from Ofu Island reveal a hemispherically heterogeneous high $^{3}He/^{4}He$ mantle, *Earth Planet. Sci. Lett.*, *264*(3), 360–374.

Jackson, M. G., S. R. Hart, J. G. Konter, A. A. P. Koppers, H. Staudigel, M. D. Kurz, J. Blusztajn, and J. M. Sinton (2010), Samoan hot spot track on a "hot spot highway": Implications for mantle plumes and a deep Samoan mantle source, *Geochem. Geophys. Geosyst.*, *11*, Q12009, doi:10.1029/2010GC003232.

Jenner, F. E., R. J. Arculus, J. A. Mavrogenes, N. J. Dyriw, O. Nebel, and E. H. Hauri (2012), Chalcophile element systematics in volcanic glasses from the northwestern Lau Basin, *Geochem. Geophys. Geosyst.*, *13*, Q06014, doi:10.1029/2012GC004088.

Johnson, K. T. M., and J. M. Sinton (1990), Petrology, tectonic setting, and the formation of back-arc basin basalts in the North Fiji Basin, *Geol. Jahrb. Reihe D.*, *92*, 517–545.

Johnson, K. T. M., J. M. Sinton, and R. C. Price (1986), Petrology of seamounts northwest of Samoa and their relation to Samoan volcanism, *Bull. Volcanol.*, *48*(4), 225–235.

Kelley, K. A., T. Plank, T. L. Grove, E. M. Stolper, S. Newman, and E. Hauri (2006), Mantle melting as a function of water content beneath back-arc basins, *J. Geophys. Res.*, *111*, B09208, doi:10.1029/2005JB003732.

Konter, J. G., and M. G. Jackson (2012), Large volumes of rejuvenated volcanism in Samoa: Evidence supporting a tectonic influence on late-stage volcanism, *Geochem. Geophys. Geosyst.*, *13*, Q0AM04, doi:10.1029/2011GC003974.

Koppers, A. A. P., J. A. Russell, M. G. Jackson, J. Konter, H. Staudigel, and S. R. Hart (2008), Samoa reinstated as a primary hotspot trail, *Geology*, *36*(6), 435–438.

Koppers, A. A. P., J. A. Russell, J. Roberts, M. G. Jackson, J. Konter, D. J. Wright, H. Staudigel, and S. R. Hart (2011), Age systematics of two young en echelon Samoan volcanic trails, *Geochem. Geophys. Geosyst.*, *12*, Q07025, doi:10.1029/2010GC003438.

Langmuir, C. H., A. Bézos, S. Escrig, and S. W. Parman (2006), Chemical systematics and hydrous melting of the mantle in back-arc basins, in *Back-Arc Spreading Systems: Geological, Biological, Chemical, and Physical Interactions*, edited by D. M. Christie et al., pp. 87–146, AGU, Washington, D. C.

Le Bas, M. J., R. W. Le Maitre, A. Streckeisen, and B. Zanettin, (1986), A chemical classification of volcanic rocks based on the total alkali-silica diagram. *Journal of petrology*, *27*(3), 745–750.

Lupton, J. E., R. J. Arculus, R. R. Greene, L. J. Evans, and C. I. Goddard (2009), Helium isotope variations in seafloor basalts from the Northwest Lau Backarc Basin: Mapping the influence of the Samoan hotspot, *Geophys. Res. Lett.*, *36*, L17313, doi:10.1029/2009GL039468.

Lupton, J. E., R. J. Arculus, F. E. Jenner, and R. R. Greene (2012), Helium isotope variations in the Northern Lau and North Fiji Basins, Abstract V23B-2820 presented at 2012 Fall Meeting, AGU, San Francisco, Calif., 3–7 Dec.

Lytle, M. L., K. A. Kelley, E. H. Hauri, J. B. Gill, D. Papia, and R. J. Arculus (2012), Tracing mantle sources and Samoan influence in the northwestern Lau back-arc basin, *Geochem. Geophys. Geosyst.*, *13*, Q10019, doi:10.1029/2012GC004233.

Macdonald, G. A., and T. Katsura (1964), Chemical composition of Hawaiian lavas1, *J. Petrol.*, *5*(1), 82–133.

Macpherson, C. G., D. R. Hilton, J. M. Sinton, R. J. Poreda, and H. Craig (1998), High $^{3}He/^{4}He$ ratios in the Manus backarc basin: Implications for mantle mixing and the origin of plumes in the western Pacific Ocean, *Geology*, *26*(11), 1007–1010.

McDonough, W. F., and S.-S. Sun (1995), The composition of the Earth, *Chem. Geol.*, *120*(3), 223–253.

McDougall, I. (2010), Age of volcanism and its migration in the Samoa Islands, *Geol. Mag.*, *147*(5), 705–717.

Millen, D. W., and M. W. Hamburger (1998), Seismological evidence for tearing of the Pacific plate at the northern termination of the Tonga subduction zone, *Geology*, *26*(7), 659–662.

Natland, J. H. (1980), The progression of volcanism in the Samoan linear volcanic chain, *Am. J. Sci*, *280*, 709–735.

Natland, J. H. (2003), *The Samoan Chain: A Shallow Lithospheric Fracture System*. [Available at http://www.mantleplumes.org/Samoa.html.]

Natland, J. H., and D. L. Turner (1985), Age progression and petrological development of Samoan shield volcanoes: Evidence from K-Ar ages, lava compositions, and mineral studies, in *Investigations of the Northern Melanesian Borderland, Circum-Pac. Counc. for Energy and Miner. Resour. Earth Sci. Ser.*, vol. 3, pp. 139–171, ed. Brocher T. M., Circum-Pac. Counc. for Energy and Miner. Resour., Houston, Tex.

Nishio, Y., S. Sasaki, T. Gamo, H. Hiyagon, and Y. Sano (1998), Carbon and helium isotope systematics of North Fiji Basin basalt glasses: carbon geochemical cycle in the subduction zone, *Earth Planet. Sci. Lett.*, *154*(1), 127–138.

Pearce, J. A., P. E. Baker, P. Harvey, and I. W. Luff (1995), Geochemical evidence for subduction fluxes, mantle melting and fractional crystallization beneath the South Sandwich island arc, *J. Petrol.*, *36*(4), 1073–1109.

Pearce, J. A., P. D. Kempton, and J. B. Gill (2007), Hf-Nd evidence for the origin and distribution of mantle domains in the SW Pacific, *Earth Planet. Sci. Lett.*, *260*(1), 98–114.

Peto, M. K., S. Mukhopadhyay, and K. A. Kelley, (2013), Heterogeneities from the first 100 million years recorded in deep mantle noble gases from the Northern Lau Back-arc Basin. *Earth and Planetary Science Letters*, *369*, 13–23.

Pelletier, B., and J.-M. Auzende (1996), Geometry and structure of the Vitiaz trench lineament (SW Pacific), *Mar. Geophys. Res.*, *18*(2–4), 305–335.

Poreda, R. J., and H. Craig (1992), He and Sr isotopes in the Lau Basin mantle: Depleted and primitive mantle components, *Earth Planet. Sci. Lett.*, *113*(4), 487–493.

Price, R. C., and L. W. Kroenke (1991), Tectonics and magma genesis in the northern North Fiji Basin. *Marine Geology*, *98*(2), 241–258.

Price, R. C., P. Maillet, I. McDougall, and J. Dupont (1991), The geochemistry of basalts from the Wallis Islands, northern Melanesian Borderland: Evidence for a lithospheric origin for Samoan-type basaltic magmas?, *J. Volcanol. Geotherm. Res.*, *45*(3), 267–288.

Regelous, M., S. Turner, T. J. Falloon, P. Taylor, J. Gamble, and T. Green (2008), Mantle dynamics and mantle melting beneath Niuafo'ou Island and the northern Lau back-arc basin, *Contrib. Mineral. Petrol.*, *156*(1), 103–118.

Salters, V. J. M., S. Mallick, S. R. Hart, C. E. Langmuir, and A. Stracke (2011), Domains of depleted mantle: New evidence from hafnium and neodymium isotopes, *Geochem. Geophys. Geosyst.*, *12*, Q08001, doi:10.1029/2011GC003617.

Shaw, A. M., D. R. Hilton, C. G. Macpherson, and J. M. Sinton (2004), The CO_2-He-Ar-H_2O systematics of the Manus back-arc basin: Resolving source composition from degassing and contamination effects, *Geochim. Cosmochim. Acta*, *68*(8), 1837–1855.

Sinton, J. M., K. T. M. Johnson, and R. C. Price (1985), Petrology and geochemistry of volcanic rocks from the northern Melanesian borderland, in *Investigations of the Northern Melanesian Borderland*, Circum-Pac. Counc. for Energy and Miner. Resour. Earth Sci. Ser., vol. 3, pp. 35–64, ed Brocher T. M., Circum-Pac. Counc. for Energy and Miner. Resour., Houston, Tex.

Sinton, J. M., R. C. Price, K. T. M. Johnson, H. Staudigel, and A. Zindler (1993), Petrology and geochemistry of submarine lavas from the Lau and North Fiji Back-Arc Basins, in *Basin Formation, Ridge Crest Processes and Metallogenesis in the North Fiji Basin*, Circum-Pac. Counc. for Energy and Miner. Resour. Earth Sci. Ser., vol. 15, pp. 119–134, eds Kroenke L. W. and Eade J. V., Circum-Pac. Counc. for Energy and Min. Resour, Houston, Tex.

Sleep, N. H. (1996). Lateral flow of hot plume material ponded at sublithospheric depths, *J. Geophys. Res.*, *101*(B12), 28,065–28,083.

Smith, G. P., D. A. Wiens, K. M. Fischer, L. M. Dorman, S. C. Webb, and J. A. Hildebrand (2001), A complex pattern of mantle flow in the Lau backarc, *Science*, *292*(5517), 713–716.

Stuart, F. M., S. Lass-Evans, J. G. Fitton, and R. M. Ellam (2003), High $^{3}He/^{4}He$ ratios in picritic basalts from Baffin Island and the role of a mixed reservoir in mantle plumes, *Nature*, *424*(6944), 57–59.

Su, Y., and C.H. Langmuir (2003), Global MORB chemistry compilation at the segment scale, Ph.D. Thesis, Department of Earth and Environmental Sciences, Columbia University.

Tian, L., P. R. Castillo, J. W. Hawkins, D. R. Hilton, B. B. Hanan, and A. J. Pietruszka (2008), Major and trace element and Sr-Nd isotope signatures of lavas from the Central Lau Basin: Implications for the nature and influence of subduction components in the back-arc mantle, *J. Volcanol. Geotherm. Res.*, *178*(4), 657–670.

Tian, L., P. R. Castillo, D. R. Hilton, J. W. Hawkins, B. B. Hanan, and A. J. Pietruszka (2011), Major and trace element and Sr-Nd isotope signatures of the northern Lau Basin lavas: Implications for the composition and dynamics of the back-arc basin mantle, *J. Geophys. Res.*, *116*, B11201, doi:10.1029/2011JB008791.

Todt, W., R. A. Cliff, A. Hanser, and A. W. Hofmann (1996), Evaluation of a ^{202}Pb-^{205}Pb double spike for high-precision lead isotope analysis, in *Earth Processes:* Reading the Isotopic Code, edited by A. Basu and S. Hart, pp. 429–437, AGU, Washington, D. C.

Turner, S., and C. Hawkesworth (1998), Using geochemistry to map mantle flow beneath the Lau Basin, *Geology*, *26*(11), 1019–1022.

Turner, S., J. Caulfield, T. Rushmer, M. Turner, S. Cronin, I. Smith, and H. Handley (2012), Magma evolution in the primitive, intra-oceanic Tonga arc: Rapid petrogenesis of dacites at Fonulaei volcano, *J. Petrol.*, *53*(6), 1231–1253.

Volpe, A. M., J. D. Macdougall, and J. W. Hawkins (1988), Lau Basin basalts (LBB): Trace element and SrNd isotopic evidence for heterogeneity in backarc basin mantle, *Earth Planet. Sci. Lett.*, *90*(2), 174–186.

Weis, D., B. Kieffer, C. Maerschalk, J. Barling, J. de Jong, G. Williams, D. Hanano, W. Pretorius, N. Mattiellie, J. Scoates, A. Goolaerts, R. Friedman, and J. Mahoney (2006), High-precision isotopic characterization of USGS reference materials by TIMS and MC-ICP-MS. *Geochemistry, Geophysics, Geosystems*, *7*(8).

Wendt, J. I., M. Regelous, K. D. Collerson, and A. Ewart (1997), Evidence for a contribution from two mantle plumes to island-arc lavas from northern Tonga, *Geology*, *25*(7), 611–614.

White, W. M. (2010), Oceanic island basalts and mantle plumes: The geochemical perspective, *Annu. Rev. Earth Planet. Sci.*, *38*, 133–160.

Woodhall, D. (1987), *Geology of Rotuma*, Miner. Resour. Dep., Minist. of Lands, Energy and Miner. Resour., *Bull. 8*, 40 pp., Suva.

Workman, R. K., and S. R. Hart (2005), Major and trace element composition of the depleted MORB mantle (DMM), *Earth Planet. Sci. Lett.*, *231*(1), 53–72.

Workman, R. K., S. R. Hart, M. G. Jackson, M. Regelous, K. A. Farley, J. Blusztajn, M. Kurz, and H. Staudigel (2004), Recycled metasomatized lithosphere as the origin of the Enriched Mantle II (EM2) end-member: Evidence from the Samoan Volcanic Chain, *Geochem. Geophys. Geosyst.*, *5*, Q04008, doi:10.1029/2003GC000623.

Wright, E., and W. M. White (1987), The origin of Samoa: New evidence from Sr, Nd, and Pb isotopes, *Earth Planet. Sci. Lett.*, *81*(2), 151–162.

Yan, C. Y., and L. W. Kroenke (1993), A plate tectonic reconstruction of the southwest Pacific, 0–100 Ma, *Proc. Ocean Drill. Program Sci. Results*, *130*, 697–709.

Zindler, A., and S. Hart (1986), Chemical geodynamics, *Annu. Rev. Earth Planet. Sci.*, *14*, 493–571.